HIGH-PRECISION ESTIMATION OF ROLL AND PITCH OF AIRCRAFTS

by

Dinesh Shenoy

Submitted in partial fulfillment of the requirements
for the degree of Master of Computer Science

at

Dalhousie University
Halifax, Nova Scotia
August 2019

I am dedicating this thesis to my family, whose sacrifices have made it possible for me to come back to the University after a gap of 10 years!!

My better-half, Preethi Pai Karkala, who stood like a rock against all the storms, faced it on my behalf and never let them affect me during the studies.

My two little sweethearts, Prathyusha Shenoy and Dhriti Shenoy, who innocently often searched for me in their bedroom, believed that I am at my work place and waited for my "return from office" lie, until we reunited.

My Aanu (dad), Prabhakara Shenoy M, who was constantly supporting me even though he felt my absence greatly.

Finally, my dearest in the world, Amma (mom), Usha P Shenoy would be super proud of me, wherever she is, always smiling and blessing me.

Table of Contents

List of Tables

List of Figures

Abstract

Positioning plays a vital role in aircraft navigation. Pitch and roll estimation are two important aspects of aircraft positioning. In our research, we focused on a low-cost pitch/roll estimation platform, which includes a low-computation processor and a small-sized memory. With the platform, we compared the performance of two pitch/roll estimation methods: complementary filter based estimation and Kalman filter based estimation. Our experimental results indicate that, between the two approaches under investigation, Kalman filter-based estimation is much more precise. In addition, we found that R matrix, a critical variable of Kalman filter, has a serious impact on convergence time and stability of Kalman filter. When the entries of R matrix are set to low values, Kalman filter-based estimation leads to faster convergence time and poor stability. When they are set to high values, Kalman filter-based estimation is more stable, but it results in slow convergence.

List of Abbreviations and Symbols Used

$1 - G(s)$	High-pass filter
A	State transition matrix of an object
A^T	Transpose of state transition matrix
$G(s)$	Low-pass filter
H	Measurement residual
H^T	Measurement residual matrix transposed
I	Identity matrix
K_k	Kalman gain
P_k	State error covariance at Time k
Q	Covariance of model noise
R	Covariance of error in sensor measurements
S_k	Measurement covariance
dt	Sample rate in Seconds
w_k	Covariance of white noise associated with state transition matrix
x_k	New state estimation
$x_k^{'}$	Previous state estimation of x_k
y_k	State vector of an object at time k
z_k	Measurement vector obtained from sensors
$P_k^{'}$	Previous estimate of P_k
AHRS	Attitude heading reference system
CF	Complementary filter
GPS	Global positioning system

KF	Kalman filter
M15pitch.Complementary	Pitch angle calculated by complementary filter in in-motion scenario with predefined angle of 15 degrees
M15pitch.Kalman	Pitch angle calculated by Kalman filter in in-motion scenario with predefined angle of 15 degrees
M15pitch.RawAccelerometer	Raw value of pitch angle calculated by accelerometer sensor in in-motion scenario with predefined angle of 15 degrees
M15pitch.RawGyroscope	Raw value of pitch angle calculated by gyroscope sensor in in-motion scenario with predefined angle of 15 degrees
M15Roll.Complementary	Roll angle calculated by complementary filter in in-motion scenario with predefined angle of 15 degrees
M15Roll.Kalman	Roll angle calculated by Kalman filter in in-motion scenario with predefined angle of 15 degrees
M15Roll.RawAccelerometer	Raw value of roll angle calculated by accelerometer sensor in in-motion scenario with predefined angle of 15 degrees
M15Roll.RawGyroscope	Raw value of roll angle calculated by gyroscope sensor in in-motion scenario with predefined angle of 15 degrees
M30pitch.Complementary	Pitch angle calculated by complementary filter in in-motion scenario with predefined angle of 30 degrees
M30pitch.Kalman	Pitch angle calculated by Kalman filter in in-motion scenario with predefined angle of 30 degrees
M30pitch.RawAccelerometer	Raw value of pitch angle calculated by accelerometer sensor in in-motion scenario with predefined angle of 30 degrees

M30pitch.RawGyroscope	Raw value of pitch angle calculated by gyroscope sensor in in-motion scenario with predefined angle of 30 degrees
M30Roll.Complementary	Roll angle calculated by complementary filter in in-motion scenario with predefined angle of 30 degrees
M30Roll.Kalman	Roll angle calculated by Kalman filter in in-motion scenario with predefined angle of 30 degrees
M30Roll.RawAccelerometer	Raw value of roll angle calculated by accelerometer sensor in in-motion scenario with predefined angle of 30 degrees
M30Roll.RawGyroscope	Raw value of roll angle calculated by gyroscope sensor in in-motion scenario with predefined angle of 30 degrees
M45pitch.Complementary	Pitch angle calculated by complementary filter in in-motion scenario with predefined angle of 45 degrees
M45pitch.Kalman	Pitch angle calculated by Kalman filter in in-motion scenario with predefined angle of 45 degrees
M45pitch.RawAccelerometer	Raw value of pitch angle calculated by accelerometer sensor in in-motion scenario with predefined angle of 45 degrees
M45pitch.RawGyroscope	Raw value of pitch angle calculated by gyroscope sensor in in-motion scenario with predefined angle of 45 degrees
M45roll.Complementary	Roll angle calculated by complementary filter in in-motion scenario with predefined angle of 45 degrees
M45roll.Kalman	Roll angle calculated by Kalman filter in in-motion scenario with predefined angle of 45 degrees
M45roll.RawAccelerometer	Raw value of roll angle calculated by accelerometer sensor in in-motion scenario with predefined angle of 45 degrees
M45roll.RawGyroscope	Raw value of roll angle calculated by gyroscope sensor in in-motion scenario with predefined angle of 45 degrees

M60pitch.Complementary	Pitch angle calculated by complementary filter in in-motion scenario with predefined angle of 60 degrees
M60pitch.Kalman	Pitch angle calculated by Kalman filter in in-motion scenario with predefined angle of 60 degrees
M60pitch.RawAccelerometer	Raw value of pitch angle calculated by accelerometer sensor in in-motion scenario with predefined angle of 60 degrees
M60pitch.RawGyroscope	Raw value of pitch angle calculated by gyroscope sensor in in-motion scenario with predefined angle of 60 degrees
M60roll.Complementary	Roll angle calculated by complementary filter in in-motion scenario with predefined angle of 60 degrees
M60roll.Kalman	Roll angle calculated by Kalman filter in in-motion scenario with predefined angle of 60 degrees
M60roll.RawAccelerometer	Raw value of roll angle calculated by accelerometer sensor in in-motion scenario with predefined angle of 60 degrees
M60roll.RawGyroscope	Raw value of roll angle calculated by gyroscope sensor in in-motion scenario with predefined angle of 60 degrees
Pitch.R0_0	Pitch angle when the R matrix was initialized with values [0,0,0,0]
Pitch.R100_200	Pitch angle when the R matrix was initialized with values [100,0,0,200]
Pitch.R25_50	Pitch angle when the R matrix was initialized with values [25,0,0,50]
Pitch.R400_600	Pitch angle when the R matrix was initialized with values [400,0,0,600]
Pitch.R800_1000	Pitch angle when the R matrix was initialized with values [800,0,0,1000]

Roll.R0_0	Roll angle when the R matrix was initialized with values 0,0,0,0
Roll.R100_200	Roll angle when the R matrix was initialized with values [100,0,0,200]
Roll.R25_50	Roll angle when the R matrix was initialized with values [25,0,0,50]
Roll.R400_600	Roll angle when the R matrix was initialized with values [400,0,0,600]
Roll.R800_1000	Roll angle when the R matrix was initialized with values [800,0,0,1000]
S15pitch.Complementary	Pitch angle calculated by complementary filter in stationary scenario with predefined angle of 15 degrees
S15pitch.Kalman	Pitch angle calculated by Kalman filter in stationary scenario with predefined angle of 15 degrees
S15pitch.RawAccelerometer	Raw value of pitch angle calculated by accelerometer sensor in stationary scenario with predefined angle of 15 degrees
S15pitch.RawGyroscope	Raw value of pitch angle calculated by gyroscope sensor in stationary scenario with predefined angle of 15 degrees
S15roll.Complementary	Roll angle calculated by complementary filter in stationary scenario with predefined angle of 15 degrees
S15roll.Kalman	Roll angle calculated by Kalman filter in stationary scenario with predefined angle of 15 degrees
S15roll.RawAccelerometer	Raw value of roll angle calculated by accelerometer sensor in stationary scenario with predefined angle of 15 degrees
S15roll.RawGyroscope	Raw value of roll angle calculated by gyroscope sensor in stationary scenario with predefined angle of 15 degrees

S30pitch.Complementary	Pitch angle calculated by complementary filter in stationary scenario with predefined angle of 30 degrees
S30pitch.Kalman	Pitch angle calculated by Kalman filter in stationary scenario with predefined angle of 30 degrees
S30pitch.RawAccelerometer	Raw value of pitch angle calculated by accelerometer sensor in stationary scenario with predefined angle of 30 degrees
S30pitch.RawGyroscope	Raw value of pitch angle calculated by gyroscope sensor in stationary scenario with predefined angle of 30 degrees
S30roll.Complementary	Roll angle calculated by complementary filter in stationary scenario with predefined angle of 30 degrees
S30roll.Kalman	Roll angle calculated by Kalman filter in stationary scenario with predefined angle of 30 degrees
S30roll.RawAccelerometer	Raw value of roll angle calculated by accelerometer sensor in stationary scenario with predefined angle of 30 degrees
S30roll.RawGyroscope	Raw value of roll angle calculated by gyroscope sensor in stationary scenario with predefined angle of 30 degrees
S45pitch.Complementary	Pitch angle calculated by complementary filter in stationary scenario with predefined angle of 45 degrees
S45pitch.Kalman	Pitch angle calculated by Kalman filter in stationary scenario with predefined angle of 45 degrees
S45pitch.RawAccelerometer	Raw value of pitch angle calculated by accelerometer sensor in stationary scenario with predefined angle of 45 degrees
S45pitch.RawGyroscope	Raw value of pitch angle calculated by gyroscope sensor in stationary scenario with predefined angle of 45 degrees

S45roll.Complementary	Roll angle calculated by complementary filter in stationary scenario with predefined angle of 45 degrees
S45roll.Kalman	Roll angle calculated by Kalman filter in stationary scenario with predefined angle of 45 degrees
S45roll.RawAccelerometer	Raw value of roll angle calculated by accelerometer sensor in stationary scenario with predefined angle of 45 degrees
S45roll.RawGyroscope	Raw value of roll angle calculated by gyroscope sensor in stationary scenario with predefined angle of 45 degrees
S60pitch.Complementary	Pitch angle calculated by complementary filter in stationary scenario with predefined angle of 60 degrees
S60pitch.Kalman	Pitch angle calculated by Kalman filter in stationary scenario with predefined angle of 60 degrees
S60pitch.RawAccelerometer	Raw value of pitch angle calculated by accelerometer sensor in stationary scenario with predefined angle of 60 degrees
S60pitch.RawGyroscope	Raw value of pitch angle calculated by gyroscope sensor in stationary scenario with predefined angle of 60 degrees
S60roll.Complementary	Roll angle calculated by complementary filter in stationary scenario with predefined angle of 60 degrees
S60roll.Kalman	Roll angle calculated by Kalman filter in stationary scenario with predefined angle of 60 degrees
S60roll.RawAccelerometer	Raw value of roll angle calculated by accelerometer sensor in stationary scenario with predefined angle of 60 degrees
S60roll.RawGyroscope	Raw value of roll angle calculated by gyroscope sensor in stationary scenario with predefined angle of 60 degrees
SD	Standard deviation

UAV	Unmanned aerial vehicle

Acknowledgements

Firstly, I would like to thank Dr.Srini, who recognized my interest in research, encouraged me to take up thesis work, and introduced me to Dr.Qiang.

Thanks to :

Dr.Qiang Ye - My supervisor, supported me throughout the tough times during the whole period of my research.

Dr.Saurabh Dey - First person who asked me, why am I not into the research field and lit the spark.

Dr.Raghav Sampangi - Valuable inputs in every meeting which was supposed to be 15 minutes long but lasted for hours.

Dr.Kirstie Hawkey - Taught me how to perform a research.

Mr.Mir Masood Ali - Wonderful friend who always stood by me, uplifted my spirits during several interruptions.

Mr.Mostafa Dafer - Unlimited inputs during my research times, especially the late night we ended up discussing about the research at the kitchen of Atlantic Superstore on Barrington Street, Halifax until 2:30 AM

Chapter 1

Introduction

Aircraft positioning is an essential task in the navigation of an aircraft. Pitch and roll estimation are part of this critical task. Technically, a pitch is an angle of an aircraft's motion in up and down direction and a roll is the angle of rotation of the aircraft in clockwise or anticlockwise direction [5]. Generally, some sensors such as an accelerometer or a gyroscope can be used to obtain the pitch and roll value. An accelerometer measures acceleration of an object in motion in relation to gravity and a gyroscope measures the rate of change of angle, also termed as the angular velocity [6]. But these sensors suffer from various errors and drifts. An accelerometer output provides accurate roll and pitch when there is no external force applied to it due to the acceleration. But, the accelerometer output suffers from errors due to extra forces and vibrations. Similarly, gyroscope sensor suffers from drift errors which is accumulated over a period of time, ultimately making it unstable in calculating the orientation of an object [6]. Hence, relying solely on the data from these sensors to estimate roll and pitch will lead to inefficient results. A promising solution is combining these sensor values and some filter (such as complementary or Kalman filter) to arrive at a high-precision estimation of aircraft roll and pitch. Technically, a filter is capable of easing the negative impact of accumulated noise and drift, ultimately helping generate more precise roll/pitch estimation.

1.1 Motivation and Challenges

Orientation estimation of an object has attracted much attention over the past years. Roll and pitch angles were calculated for several objects such as Unmanned Aerial Vehicle (UAV) [7], walking robots [8], biomedical applications [9] and motion trackers [10]. These prior researches used magnetic sensors to measure the magnetic

field of the earth and a set of inertial sensors such as an accelerometer and a gyroscope to measure gravity and angular velocity, respectively. A few researchers have used Attitude Heading Reference System (AHRS) for roll and pitch angle estimation which uses rate gyroscope and gravity sensors. But these sensors are prone to errors when low quality AHRS or sensors are used to lower the cost of hardware platform [11]. Other than these sensors, GPS sensors were successfully used in developing a low-cost system [12], [13]. These studies used an ad-hoc non-linear vector matching algorithm along with complementary filter for roll and pitch angle determination [14]. The vector matching algorithm was initially proposed in the description of Wahba's problem [15], mainly for satellite attitude estimation to track stars. Attitude estimation is an another term used for calculating positioning of an object with respect to its angle and location. This research was further extended in several studies [16], [17] where a Kalman filter was used in roll and pitch angle determination. Kalman filter was proposed by Rudolf E. Kalman in 1960 [18].

One problem with the existing schemes based on accelerometer and gyroscope is that they often require a high-end computation platform to obtain high precision. In our research, we attempted to propose high-precision roll/pitch estimation methods for low-cost platforms that involve a slow processor and a small memory. Technically, the proposed estimation algorithms are based on a complementary or Kalman filter. Complementary filters can be configured as a low-pass or a high-pass filter to eliminate the noise from the sensors [3]. Kalman filter is a recursive filter which saves the previous state to measure and estimate the current state of an object. By proposing a low cost platform to obtain a high precision roll and pitch angle, our research achieves a better accuracy using complex approaches.

1.2 Contributions

In this thesis, we present two high-precision roll and pitch estimation methods for aircrafts: one is based on a complementary filter and the other is based on a Kalman filter. The performance of the proposed schemes were thoroughly analyzed to illustrate their advantages and disadvantages. Note that, in our research, we focused

on algorithms for low-cost platforms, which include a slow processor and a small memory. As a result, the hardware platform used in our research includes a 3-axis digital accelerometer and a 3-axis digital gyroscope installed on a Cypress CYBLE module. This is a fully certified module that can be used for wireless communication with a processing frequency of 52Hz.

When the Kalman filter was studied in depth, a measurement error covariance matrix was found to have a serious impact on the performance of the filter. Officially, this matrix is called as R matrix with which the trustworthiness of the sensor measurements can be tweaked. An in-depth analysis of this matrix is included in this thesis, illustrating the impact of R matrix on the precision of the proposed roll/pitch estimation schemes.

1.3 Thesis Outline

The rest of the thesis is organized as follows. Chapter 2 covers all the background information required to understand the details of the research explained in this thesis. It sheds light on the roll and pitch angles of an aircraft, the role of sensors in detecting these angles followed by the importance of sensors to estimate the precise roll and pitch angles. Chapter 3 gives the information about previous research work in this area. It has separate sections covering previous work with the complementary filter, the Kalman filter, as well as few hybrid approaches where these filters are integrated together. This chapter also covers the limitations of the existing studies. Chapter 4 explains the methodology used in this research work such as the hardware setup, the experimental scenarios along with the procedure of data collection and finally the data analysis strategies used in the research. Followed by this, the Chapter 5 shows all the experimental results. Finally, Chapter 6 draws conclusions from this research and describes future work directions.

Chapter 2

Background

2.1 Roll and Pitch Determination

Kinematics is the branch of mechanics which describes about the motion of an object [19]. Different models of kinematics are required in control and analysis of many systems such as cranes, satellites and other vehicles [20]. A controlled motion of these systems can be performed to achieve different categories of tasks [5]. Aircraft can be considered as one of the system having kinematics behaviour and the orientation of aircrafts can help in understanding the flight navigation. Orientation of any object can be commonly described using the Euler angles and roll-pitch-yaw angles, calculated based on a given rotation matrix [21] [5]. Roll, pitch and yaw angles are shown in the figure 2.1 below, where an object is represented with three axes. Roll can be described

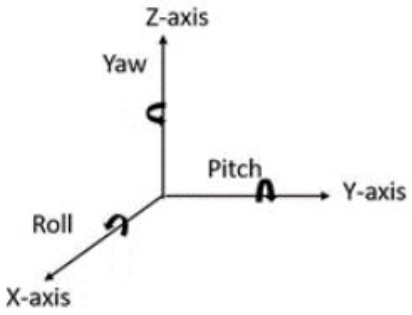

Figure 2.1: Roll, pitch and yaw angle representation
Source : Adapted from [1]

as the change in the angle of an object in X-axis. Roll angle for an aircraft is shown in the below figure 2.2 For an aircraft, roll is the angle of rotation in clockwise and anticlockwise direction. Pitch can be described as the change in the angle of an object in Y-axis. Pitch angle for an aircraft is shown below figure 2.3 In this research work, we have concentrated on calculating roll and pitch angles for an aircraft based on the

Figure 2.2: Roll image for an aircraft
Source : Adapted from [2]

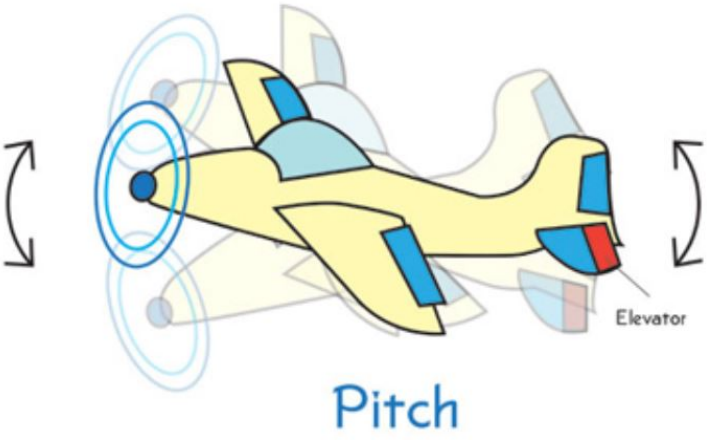

Figure 2.3: Pitch image for an aircraft
Source : Adapted from [2]

hardware setup we chose to perform the experiments. The hardware setup mainly consists of different types of sensors to measure the roll and pitch angles. The sensors which can be used to calculate these angles is explained in the below section. These sensors can be either used individually or their readings can be integrated to calculate pitch and roll angles of an object.

2.2 Sensors and Their Roles

Different types of sensors are used to capture the movement, acceleration and rotation of an object thereby calculating the orientation. Individual sensors as well as multiple sensors can be integrated to measure orientation of an object. Few sensors that were used in some of the previous experiments are explained below. One of the way with which pitch and roll can be measured is using the tilt sensor which utilizes earth's gravitational field [22]. Some of the tilt sensors include fluid based sensors and an accelerometer. Another experiment utilized multiple gyroscopes and an inclinator [8]. Even though the aim of the experiment was to develop a walking robot, pitch and roll angles were calculated to help the motion of the robot. A research implemented a tilt compensated eCompass using accelerometer and magnetometer sensors [23]. Even the related work section covers several previous research performed in the field of calculating roll and pitch angles utilizing these sensors. Accelerometer measures the acceleration of a moving object based on earth's gravity [24]. Gyroscope measures rate of angular velocity [25]. A magnetometer measures the earth's magnetic field [23]. But, usually the individual or integrated sensor raw values will contain noise due to several factors. For instance, an accelerometer suffers from errors due to the force of acceleration and a gyroscope suffers from drift errors [1]. Hence, filters are used to remove these errors (noise) and achieve better results.

2.3 Filters

Several filters are available with past research work to eliminate the noise from sensor measurements. Complementary filter is a simplest form of a filter which involves less calculations, hence quick to produce the results [3]. Kalman filter, proposed by R. E. Kalman in 1960 [18], later improved in the next year with R. S. Bucy [26]

is a complex algorithm compared to complementary filter provides better accuracy. These filters are explained in detail in below sections.

2.3.1 Complementary Filter

A complementary filter is the simplest form of filter which can be configured to work on various sensor measurements to eliminate the noise and obtain desired result. When there are multiple sensors such as accelerometer and gyroscope, a complementary filter can perform a low-pass filtering on one sensor value and a high-pass filtering on the other to integrate and produce a better output than the raw sensor values [27]. A basic complementary filter is shown in below figure 2.4 If x

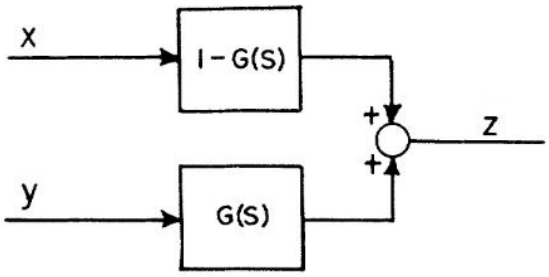

Figure 2.4: Basic complementary filter presented in [3]

and y are two noisy sensor measurements, a basic complementary filter can be fed with these measurements to obtain a result of z. Among x and y, if noise in y is of higher frequency compared to the noise of x, then G(s) can be made as a low-pass filter to remove high-frequency noise from y. When G(s) is configured as low-pass, the complement of it is 1-G(s) becomes a high-pass filter. This high-pass filter can be used to remove the low-frequency noise from signal x. This is shown in the figure 2.5 below. As the accelerometers suffers from high noise created due to acceleration [28], sensor measurements of accelerometer can be fed into a low-pass filter. Gyroscope suffers from small drift errors which gets accumulated over time [1]. Hence, gyroscope sensor measurements can be fed into a high-pass filter. Integrating these readings can result in pitch and roll angle of an object. If pitch and roll angles of an aircraft are considered as decoupled processes, the accelerometer and gyroscope sensor data can

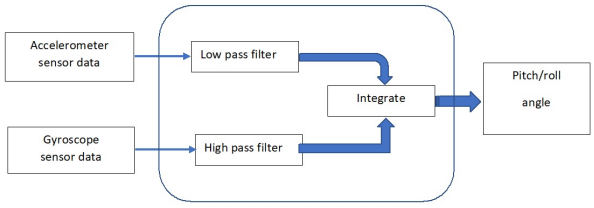

Figure 2.5: Complementary filter on accelerometer and gyroscope sensor measurements as shown in [1]

be filtered separately which is a linear complementary filter [29]. If a magnetometer sensor is available in the hardware setup, then a non-linear complementary filter can be implemented with additional mathematical calculations [30], [31]. The flowchart to explain the operation of simple linear complementary filter in detail is given in below figure 2.6 The sample rate is the input at which sensor measurements are

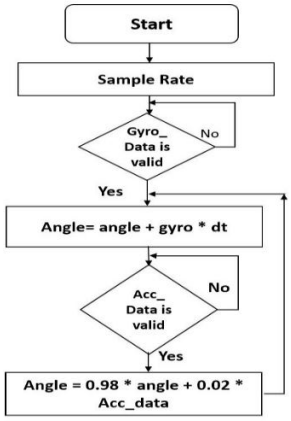

Figure 2.6: Flow chart of complementary filter as shown in [1]

fed into the complementary filter. Gyroscope sensor data is given more preference, hence it is passed through a high-pass filter by giving more preference to it (98%). Accelerometer sensor data which has high noise is passed through a low-pass filter. Integrating these sensor measurements based on the axis of rotation can give us pitch or roll angle of an object.

2.3.2 Kalman Filter

Kalman filter is a powerful tool for combining information where there is high uncertainty [32]. It is an iterative filter which uses the measurements from sensors, uses few mathematical calculations including matrices and the previous state to measure the current state. Overall picture of Kalman filter along with its details in every step is wonderfully explained in the tutorial by T. Lacey and N. Thacker [4].

The process of putting all the steps of Kalman filter is termed as building a model of the object whose orientation is being calculated. The block diagram of Kalman filter operation is described in figure 2.7 below.

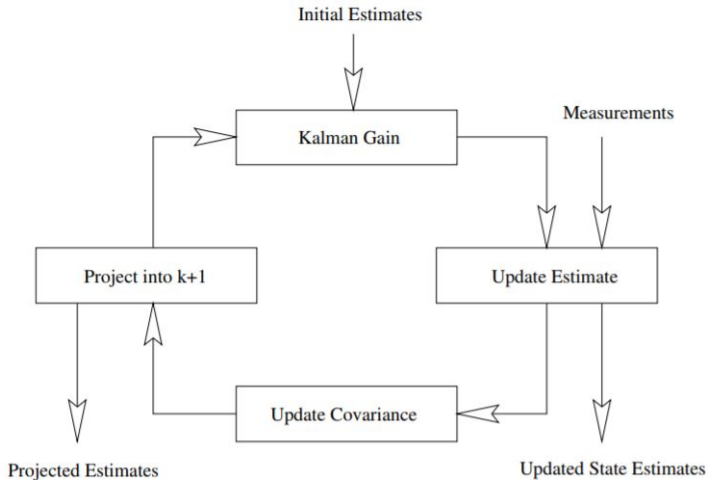

Figure 2.7: Operation of Kalman filter as described in [4]

The initial estimates are few matrices used in the state (roll/pitch) calculations, explained ahead in this section. Using the initial estimates and the latest sensor measurements the current state is estimated. The covariances of the current state and measurements, saved as matrices are also updated after calculating the new state. Kalman gain is calculated which depicts the overall operations and helps in weighing the measurements and model together. All the formulae and explanations are retrieved from the Kalman filter tutorial by T. Lacey and N. Thacker [4].

Let us consider we want to calculate state of an object 'y' , it can be represented with the following formula :

$$y_{k+1} = Ay_k + w_k \tag{2.1}$$

where; y_k is state vector of the object at time k, A is the state transition matrix of the object from state k to k+1; w_k is the associated white noise process with a covariance represented with a matrix. The state transition matrix represents the dynamics of the system. For a flying object like an aircraft, it can be represented with a 3X3 matrix to explain 3 dimensions of the aircraft. Before incorporating the measurements, Kalman gain K_k is calculated based on the initial estimates.

$$K_k = P_k^{'} H^T {S_k}^{-1} \tag{2.2}$$

P_k is the state error covariance matrix at time k. $P_k^{'}$ is the previous estimate of P_k. H is a matrix called as measurement residual, maps a state onto measurements. S_k is a measurement covariance matrix which depends on the covariance of previous model predictions transformed into measurements.

$$S_k = H P_k H^T + R \tag{2.3}$$

H^T is the H matrix transposed. R is the covariance matrix of error in sensor measurements. This matrix is a 2X2 matrix which can be varied based on the determination of noise of sensor measurements.

Using the Kalman gain and the measurements, new state estimation x_k is done using a prior estimate $x_k^{'}$. At this step, measurement residual - H matrix is used along with a measurement vector Z_k.

$$x_k = {x_k}^{'} + K_k(z_k - H x_k^{'}) \tag{2.4}$$

For an aircraft, a roll or pitch angle can be measured based on the gravity vector by using atan2 function in mathematical library applied upon the accelerometer and gyroscope sensor measurements. This is called as a measurement vector Z.

Once the current state is estimated, state error covariance matrix is updated based on the calculated Kalman gain and previous state error covariance matrix.

$$P_k = (I - K_k H) P_k^{'} \tag{2.5}$$

I is called as an identity matrix which has all the entries as zero except the diagonal entries as 1. As a next step, state projection x_{k+1} is achieved using the estimated

state x_k and the state transition matrix Φ.

$$x_{k+1} = \Phi x_k \tag{2.6}$$

At this stage, the Kalman filter model has the latest state estimates using the previous estimates and new sensor measurements. Now, an update to the state error covariance matrix is performed as Kalman filter is an iterative filter which saves all these values for future calculation. This step uses the model noise that is being built along with state transition matrix Φ as follows:

$$P_{k+1} = \Phi P_k \Phi^T + Q \tag{2.7}$$

Φ^T is the state transition matrix transposed. Q is the matrix representing the covariance of model noise. This P_{k+1} matrix is used as P_k in the next step while measuring the Kalman gain. Overall, there are five matrices that are used in the Kalman filter. They are P (state error covariance matrix), H(measurement residual), R(covariance matrix of error in sensor measurements), Q(covariance of model noise) and I(identity matrix). Each matrix can be initialized with predefined values as explained in the several previous researches [33], [34], [35], [36] and they are updated in every cycle of Kalman filter as the algorithm is iterative.

Description	Equation
Kalman Gain	$K_k = P'_k H^T \left(H P'_k H^T + R\right)^{-1}$
Update Estimate	$\hat{x}_k = \hat{x}'_k + K_k \left(z_k - H\hat{x}'_k\right)$
Update Covariance	$P_k = \left(I - K_k H\right) P'_k$
Project into $k+1$	$\hat{x}'_{k+1} = \Phi \hat{x}_k$ $P_{k+1} = \Phi P_k \Phi^T + Q$

Figure 2.8: Summary of Kalman filter algorithm [4]

The recursive nature of Kalman filter algorithm is summarized in the above figure 2.8, which provides the four steps and their corresponding formulae. Due to the recursive nature of Kalman filter algorithm, which uses previous state and current state estimates along with several covariance matrices, the accuracy of this algorithm is very high compared to the complementary filter discussed in the section 2.3.1. On

the contrary, due to several mathematical calculations, the Kalman filter is computationally heavier than the complementary filter [37], [38].

Chapter 3

Related Work

There are various researches in the field of aviation which measures the object orientation using several types of filters. There are various implementations of complementary filter along with UAV (Unmanned Aerial Vehicle), linear and non-linear implementations of Kalman Filter along with inertial system in a virtual environment, time varying Kalman filter to achieve positioning using gyroscope are to list a few of them. This chapter covers the literature review of the complementary filter, Kalman filter and hybrid approaches to calculate the orientation of an object by previous researches. Hybrid approaches are the researches which either used multiple filters in parallel or integrated the results of one filter as an input to an another filter. This chapter also covers the limitations of these past researches with respect to calculating roll and pitch angle of an aircraft.

3.1 Complementary Filter Based Approaches

Complementary filter is one of the simple filters which incorporates a low-pass and a high-pass filter as explained in chapter 2.3.1 above. A low-pass filter can be applied to the sensor values with higher error rate. A high-pass filter is applied to sensor values with lower error rate [3].

A research from 2008 explained an implementation of non-linear complementary filter for determining positioning of a UAV (Unmanned Aerial Vehicle) [27]. Non-linear complementary filter was proposed in this research as the UAV makes sharp turns which creates severe error rate in accelerometer sensor output. Authors used accelerometer and gyroscope sensor values to obtain low frequency and high frequency positioning. To eliminate the errors due to sharp turn of UAV, the pitch rate measured by gyroscope was used in some of the previous research work [39], [38]. The non-linear

complementary filter was tested from previously available data of a fixed wing UAV from the Australian Center for Field Robotics, University of Sydney. The result of the proposed filter was compared with the output from a GPS/INS Kalman filter [40] which was considered as the baseline. The proposed algorithm with this paper is very low in complexity which is ideal for low powered devices. This paper also points out the drawback of Kalman filter in certain scenarios where the accelerometer is producing invalid sensor values.

Tae Suk Yoo and his team implemented a version of complementary filter called gain-scheduled complementary filter for a MEMS based attitude and heading reference system such as a UAV [37]. This research can efficiently replace several versions of Kalman filter such as extended Kalman filter which are very complex to implement [41], [42], [43] as well as the simple filters such as SISO (single input single output) filters [44], [45], [46], [47]. The main aim of this research work was to cover the cases of UAV when the accelerometer sensor stops giving valid readings. This happens when the UAV is circling for a very long time where it is affected by both the centrifugal force as well as the gravitational acceleration resulting in invalid SISO filter output [48]. The roll and pitch angle of UAV is calculated using a IMU with magnetic sensor in the scenarios such as non-acceleration, low and high-acceleration [49], [50], [51].

Another research proposed couple of versions of complementary filter to measure the attitude and gyroscope bias estimation of an unmanned aerial vehicles [52]. Both the proposed filters work on special orthogonal group SO(3). Inspired from some of the previous works with complementary filter on SO(3) [30], [31] authors of this research came up with a direct complementary filter and a passive non-linear complementary filter. Direct complementary filter measures the attitude of quaternion rotations of SO(3). Passive non-linear complementary filter overcomes the disadvantages of direct complementary filter such as complex implementation and high sensitivity to noise.

R.Kottath et al. proposed an advanced complementary filter approach to determine roll and pitch angles of an unmanned aerial vehicle [53]. This study used

accelerometer, gyroscope and magnetometer sensors to estimate the orientation. The interesting part of this work was modifying the behaviour of the complementary filter. Usually, a complementary filter adjusts the weights on the sensor output and merges them to obtain roll and pitch angles. The weight on the sensor output remains constant throughout the operation of the filter. This study proposed the weight adjustment of sensors in every cycle of the complementary filter operation based on MMAE based adaptive Kalman filtering scheme [54], [55]. This scheme allows to estimate an angle, and update the estimate based on the output calculated from sensors.

3.2 Kalman Filter Based Approaches

Kalman filter was proposed by Rudolf E. Kalman in 1960, has iterative steps to calculate desired result based on predict and update steps [18]. This filter predicts the future data based on the existing data. The filter starts with an initial set of values along with sensor values fed to it to obtain a new value. Before obtaining the new value, few predictions are made which are updated after the new value is calculated. Hence, it is an iterative filter and the covariances are calculated at every step and they are used in the future steps [56]. This helps to obtain better efficiency and accuracy on the unknown values that are calculated using the Kalman filter, which is pitch and roll angles in our case.

One of the oldest research paper from the year 1975 by Walter T Higgins gives basic distinction between complementary filter and Kalman filter [3]. This paper explains that the complementary filter is a type of a Kalman filter. As a low-pass and a high-pass filter, complementary filter utilizes the sensor values fed to it and estimates the result. It does not save any information about the current state. On the other hand, the Kalman filter always saves the current state and the errors in the current state. This helps Kalman filter to accurately measure the results in the further steps as it already has the error rate and previous state. Several examples of implementation of Kalman filter and complementary filter along with digital implementation is also given in this paper.

Demoz Gebre-Egziabher and his team performed a research in 1996 about a time-varying Kalman filter used on gyroscope and magnetic field sensors along with low pass filters [11]. This paper addresses the common issue with gyroscope sensors – the drift errors, and also explains how to eliminate them using time-varying Kalman filter. Time varying Kalman filter helps in determining attitude of an aircraft using a single GPS baseline in combination with ad-hoc non-linear acceleration vector algorithm applied on gyroscope sensor data to eliminate the drift errors [57], [58]. An interesting study was carried out by Eric Foxlin to fulfil the need of an accurate and quick responding head-tracking system [59]. A Kalman Filter implementation is explained here, using two kind of sensors: gyroscope and gravimetric inclinometers to achieve head-tracking of an inertial system in a virtual environment. Even though this paper is not directly related to aircraft pitch and roll, it sheds some light on a different type of an implementation of Kalman Filter using gyroscope values [60]. This research also explains how the drift of gyroscope sensor can be avoided by fine-tuning the Kalman filter while estimating the orientation of a flying object where there are rapid turns [61].

Another research from 2008 used accelerometer, gyroscope and GPS sensor values to measure the orientation of a device in motion [62]. The devices that were experimented contained all these three sensors in models such as miniature air vehicles. The gyroscope values were used to measure time propagation and the accelerometer and GPS sensors are used to measure the Kalman gain portion of Kalman filter [63], [46]. A vector arithmetic approach was adopted using all these three-sensor values to calculate Euler attitude vector error [64]. There was a reset of measurement values after each update followed by the calculation in repetition [65]. This helps in eliminating the errors and get accurate orientation of an aircraft. The testing of algorithm was done using a flight simulation containing several scenarios such as testing in loops and circles.

A slightly off-topic research is about GPS or INS integration using a direct Kalman

filter [66]. Even though it is not directly related to this research, this paper explains about another implementation of a Kalman filter on GPS sensor readings [67]. Kalman filter normally records the errors of sensor values (also known as Kalman Gains) fed to it and uses them in the further steps to estimate the results. But, this is computationally very costly as the previous Kalman Gains are used in every calculation along with calculating Kalman Gains in the current cycle as well. This paper proposes a direct Kalman filter implementation with a two stage estimator method to track the Kalman Gains which reduces the load on calculations [68], [69].
Another research concentrated on attitude estimation of a moving device based on inertial and magnetic sensors using a quaternion-based indirect Kalman filter [6]. The magnetic sensor values are used only to calculate yaw angles by combining multiple values. The acceleration of the device is calculated using the Kalman Gain which sufficiently decreases the load on accelerometer and corresponding errors. Even though this paper describes about yaw angles which is not the topic of interest in this research, the yaw angles can be calculated easily using gyroscope sensor values. Hence, using indirect Kalman filter implementation and yaw angles, there is a possibility to enhance the existing algorithm to obtain better pitch and roll values.

3.3 Hybrid Approaches

There are various research work which utilized multiple filters to calculate the orientation of an object. Some of them utilized complementary filter and Kalman filter together where as some used Kalman filter filters multiple times to filter the noise and achieve orientation.

An interesting research by Cao Dong and his team utilized Kalman filter and complementary filter to calculate attitude angles of a UAV [70]. MEMS (microelectromechanical system) gyroscope was used in the research as it is cost effective and small in size [71] along with accelerometer. But the MEMS gyroscope sensor suffers from white noise and drift errors. Kalman filter was used to eliminate the noise and errors [72], [73]. Complementary filter was used to fuse the result from Kalman filter along with an accelerometer and a GPS sensor readings to obtain the roll and pitch

angles of the UAV. The validation of results in this research utilized simulation from MATLAB tools.

Another hybrid approach was to cascade two Kalman filters together to calculate the orientation of human body segment using MEMS-IMU [74]. Even though this research is not directly related to current topic, the tilt angles of a human body is measured using Kalman filters which is the area of interest. According to authors, the older experiments utilized Kalman filters along with utilization algorithms such as QUEST [75], O2OQ [76] and G-N [77] to estimate the orientation using accelerometer, magnetometer and gyroscope sensors. But the problem with this approach is when the accelerometer and magnetometer are unavailable then filter output will yield the optimal result [76]. Another approach to calculate the orientation of an object is by using a complementary Kalman filter approach in two dimension and three dimension orientation [78], [31]. This research proposed a faster and a cascaded Kalman filter approach, where, the algorithm uses two linear Kalman filters. First Kalman filter calculates tilt angles using accelerometer [79]. The result of first step is further used by a second Kalman filter to calculate the yaw angle. In this way, orientation of an object can be found in a two step process.

3.4 Contributions of the Proposed Schemes

As explained in the previous sections of this chapter, the literature review of the filters used in the area of object orientation detection showed the vast amount of researches mainly concentrated on UAVs and quadrocopters. The pitch and roll detection specific to aircrafts was not available. However, these schemes do not work well with low-cost platforms consisting of a simple processor and a small memory. As the existing schemes used several sensors along with high end computation platforms, a lot of data from sensors was generated. This resulted in operation overhead of data synchronization to generate roll and pitch angles. A lot of these previous researches utilized simulators to test the performance of the filters. T.Islam et al. [1] produced a comparison of the complementary and the Kalman filter for an AHRS. The experiment included quaternion rotations to capture the roll, pitch and yaw using an

Arduino based hardware setup. From the results, it was clear that the experiment was performed in stationary mode as the raw accelerometer data is in tandem with pitch and roll calculated with complementary and Kalman filter. Also, the quaternion rotations were not fixed, and they were random. The baseline used for calculating the roll and pitch angles were also not very clear.

This thesis extends the comparison to a in-motion setup and compares these filters to understand which filter is more efficient and accurate. This research is directly applied towards pitch and roll angle estimation for light weight aircrafts with a seating capacity of 20 or less. This thesis also sheds light on a behaviour of the Kalman filter where the trust on sensor measurements are altered based on testing conditions. Along with a selection of a predefined angles, a set of values were configured to understand the roll and pitch angle output. This part of the thesis can help in understanding the time convergence and the stability of the Kalman filter in different testing conditions that can be modified based on the application of the Kalman filter.

Chapter 4

Methodology

This chapter gives a complete coverage of the research work and the methodologies applied in performing the experiments to obtain the results. The objective of this thesis is to obtain higher precision aircraft positioning such as roll, and pitch based on the efficiency and accuracy of complementary filter and Kalman filter. There was a comparison of complementary filter and Kalman filter based on accelerometer, gyroscope and magnetometer data to capture roll, pitch and yaw of an aircraft [1]. The comparison included the roll and pitch calculated using complementary filter and Kalman filter along with raw data of accelerometer and gyroscope in stationary mode only with no movements. Hence, we decided to extend this research by comparing these filters in both stationary as well as in-motion. While exploring the Kalman filter implementation, we extended our research also to a measurement error covariance matrix - R matrix. It is a 2X2 matrix which helps in determining the error covariance from sensor measurements. Our experiment contained accelerometer and gyroscope sensors which might contain the error covariance. So, we inspected the R matrix with various values to get the best precision values for the Kalman filter. Hardware configuration section covers the hardware setup information along with other tools used in this research. In this section, we cover all the steps of the experiments performed along with answers such as why and how. Data collection and sampling sections cover how the data was gathered and inspected along with the reasons behind the decisions of data evaluation. Finally the data analysis section explains how the sampled data was evaluated to reach a conclusion of the research.

4.1 Hardware Configuration

The hardware setup included a Cypress CYBLE-014008-00 module incorporated with LSM6DS3 which is a 6-degrees of Freedom inertial measurement unit (IMU). This IMU contains a 3D digital accelerometer (ADXL345) and 3D digital gyroscope (ITG-3205). This whole setup consumes very less power with a low cost to build. The Kalman filter and the complementary filter algorithm were implemented on this IMU. Below figure 4.1 shows the hardware setup used for this research work.

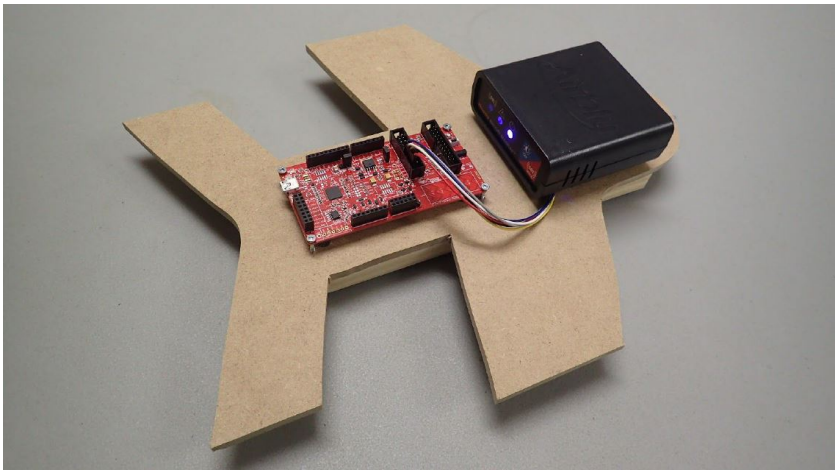

Figure 4.1: Hardware setup containing accelerometer and gyroscope sensors

Even though the primary aim of the research was to calculate roll and pitch angles, fine tuning of R matrix to understand its impact on Kalman filter was the first step in getting a higher precision roll and pitch. Hence, first phase of research and experiment was performed to calculate roll and pitch angles based on different values of R matrix. Using the result of this experiment, comparison of complementary filter with Kalman filter was performed by calculating roll and pitch angles in stationary and in-motion scenarios.

Figure 4.2 gives a brief description about the hardware module we used for the experiments. It has a 32-bit processor with a single cycle, operating upto 48 MHz. Hence, it is a low powered microcontroller with a limited processing capacity. The memory is also limited with 128 KB of flash memory and 16 KB of SRAM memory. It is clear from the module description that hardware has a slow processor and a

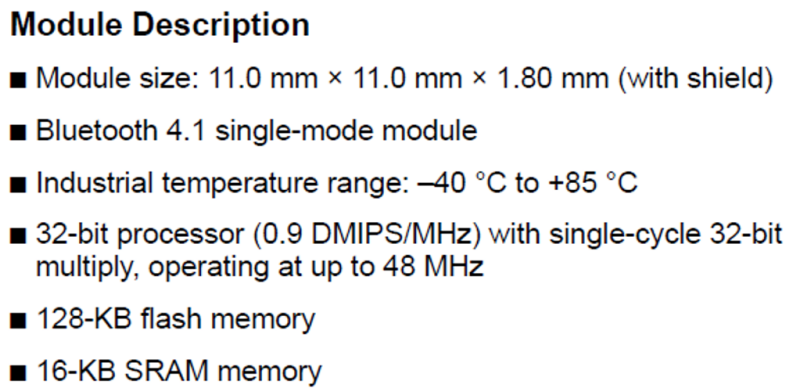

Figure 4.2: Module description

limited memory.

We used a toy train to place the IMU in different angles and obtained the measurement. The roll and pitch values were captured while the toy train was kept stationary as well as in-motion with different angles. The main requirement to use a toy train was to obtain the errors in accelerometer and gyroscope sensors at different angles with a movement. Stationary position will not have any impact on the sensors, but the objective of the thesis is to eliminate the errors from sensors when there is a movement. Ideal testing would have been in a real world scenario by generating the errors in sensors through an actual aircraft. But, as it is a very expensive procedure, we required a method to generate errors during motion. Initially we looked into using a toy plane for in-motion scenarios. But the main problem with it was not knowing the actual angle at which the toy plane flies to estimate the predefined angle and behaviour of complementary and Kalman filter. Also, the size of toy plane was so small that we would not be able to house our hardware setup on it. Hence, we chose a toy train where we could set up a predefined angle, generate errors in sensors by moving the toy train and estimate the behaviour of filters. This experimental setup helped us to estimate the performance of both filters by considering predefined angle as a baseline.

The calculation of angles at which experiment was performed were measured using an iOS application – "Compass". This application gives us the different angles based on the position of iPhone along with its inbuilt sensors. When the results are available,

the accuracy can be measured in the form of time in seconds taken by each algorithm to reach respective angles.

4.2 R Matrix Evaluation

The research was categorized into two phases, the first step was to understand the effect of R matrix in the Kalman filter behaviour for the hardware setup used. Data collection procedure along with data analysis and the experiment setup details are covered in below sections.

4.2.1 Experiment Details

To evaluate the effect of different values of R matrix on a Kalman filter, a fixed angle of 45 degrees was chosen. This angle is just an example to portray the behaviour of Kalman filter. The initial plan was to test Kalman filter behaviour with 10 to 20 values of R matrix. But, as we were using a low powered hardware setup containing a small microcontroller with a limited processing power and low memory, we could run only 5 instances of Kalman filter simultaneously. Running simultaneous executions of Kalman filter was the step to make sure to use the same raw roll and pitch angles to understand the behaviour of Kalman filter and the processing of the filter was also done on the same hardware setup. The five different values of R matrix were selected based on several previous experiments [33], [34], [35], [36].

After carefully evaluating different angles for roll and pitch calculation, the final angle at which this experiment performed was at 45 degrees. The choice of 45 degrees is just an example to understand the behaviour of the Kalman filter with different R matrix values. Being a 2X2 matrix, we finalized on 5 different values for the matrix to understand the precision.

(i) [0,0,0,0]

(ii) [25,0,0,50]

(iii) [100,0,0,200]

(iv) [400,0,0,600]

(v) [800,0,0,1000]

The first set of values (0,0,0,0) were selected to understand the precision of roll and pitch values when the R matrix was completely eliminated. The second (25,0,0,50) and third (100,0,0,200) set of values were selected to slowly increase the sensor measurement error covariance and understand its effect on the precision of output on Kalman filter. The final two values (400,0,0,600) and (800,0,0,1000) were selected to understand how the Kalman filter behaves when the sensor measurement error covariance becomes very high. All these five set of values were short-listed based on the experiments listed in prior research [33], [34] in combination with the behaviour of IMU used for this experiment.

Overall, we obtained 10 different results from this experiment to understand the effect of R matrix on the roll and pitch angle precision.

4.2.2 Data Collection

For the R matrix evaluation, only Kalman filter algorithm was activated in the IMU as the R matrix is a part of the Kalman filter. IMU was fixed on a toy-train with a predefined angle of 45 degrees. The predefined angle of 45 degrees was chosen just as an example to perform this experiment. The objective of this experiment was to analyze the behaviour of Kalman filter with sensor errors irrespective of its angle. Hence, the assumption is the Kalman filter would behave in similar terms with other angles as well. The different values of R matrix mentioned in the section 4.2.1 were configured in the Kalman filter implementation. As the Kalman filter is a complex algorithm, even though the IMU was capable of driving the sensors at operating frequency of 52Hz, we had to reduce the it to incorporate 5 simultaneous executions of the Kalman filter. Along with the single round of a roll followed by a pitch experiment, all the R matrix values were tested using separate executions of the Kalman filter algorithm. This helped in obtaining unanimous behaviour of the Kalman filter for different R matrix values on a single capture of raw sensor values.

The R matrix can manipulate the behaviour of Kalman filter algorithm in 2 ways [4]. The time of convergence to a particular predefined angle changes with the different values of R matrix. Also, the sensitivity of Kalman filter output varies when these

values of R matrix differs. Hence, the time convergence along with the sensitivity of roll and pitch angles were analyzed using the results of this experiment. The IMU affixed on a toy train was used to perform the experiment. The noise and errors in the sensors were obtained by moving the toy train in different paths. The predefined angle of 45 degrees was obtained using the native application of an Apple smartphone, shown in figure 4.2. Overall, for each roll and pitch experiment, 5 different Kalman filter angles were obtained which were further analyzed for the effect of different R matrix values. The time taken by each Kalman filter algorithm based on its R matrix values were captured along with the actual roll and pitch angles. Standard deviation was used as a measure to estimate the sensitivity of Kalman filter. These values were listed using the table explained in the next section.

4.2.3 Data Analysis Method

The results obtained from the R matrix evaluation is first stored in a table, shown in table 4.1 for further investigation. Along with the pre-defined angle of 45 degrees, five different values of R matrix were configured in five separate executions of the Kalman filter. Five simultaneous executions of Kalman filter were performed to make sure the R matrix evaluation is made on the same set of raw sensor roll and pitch angles.

R matrix [2X2] values	Predefined angle	Convergence time for Kalman filter (in seconds)	Standard Deviation $\sqrt{\frac{1}{N}\sum_{i=1}^{N}(x_i - \overline{x})^2}$
[0,0,0,0]	45		
[25,0,0,50]	45		
[100,0,0,200]	45		
[400,0,0,600]	45		
[800,0,0,1000]	45		

Table 4.1: R matrix evaluation table

Convergence time field explains the time taken by Kalman filter for each R matrix value to reach the predefined angle of 45 degrees. Standard deviation (SD) of the data

set was calculated for each Kalman filter execution to understand amount of distribution of the output (angle) for each R matrix value. SD also helped in understanding sensitivity of Kalman filter.

The comparison of every entry from the third, fourth and fifth column helped in determining the effect of R matrix values to obtain best precision in the hardware setup used for this experiment. This data was also plotted using matlab graphs which is shown in the experimental results section.

4.3 Comparison of Complementary and Kalman Filter

The second step of the research was to evaluate the performance of the complementary filter and Kalman filter algorithm and compare the roll and pitch angles. As mentioned in the section 4.2.2, raw sensor data was readily available from both the accelerometer and gyroscope sensors at the rate of 52 Hz. The complementary filter was implemented as a low-pass and a high-pass filter to eliminate the errors of sensors and obtain roll and pitch angle. The Kalman filter used a recursive approach to eliminate the noise from sensors and calculate roll and pitch angle [3]. Other than this, the raw values from the sensors along with a predefined angles were utilized as the baseline for roll and pitch calculations.

4.3.1 Experiment Scenarios

As we obtained the optimal values of R matrix, the next set of experiments to compare the performance of complementary and Kalman filters were performed in two major steps, each step containing 4 different scenarios.

The two steps were :

(i) Stationary

(ii) In-motion using a toy train

The 4 different scenarios for the roll and pitch measurement were as follows:

1. When the IMU module is at 15 degrees with respect to roll and pitch
2. When the IMU module is at 30 degrees with respect to roll and pitch
3. When the IMU module is at 45 degrees with respect to roll and pitch
4. When the IMU module is at 60 degrees with respect to roll and pitch

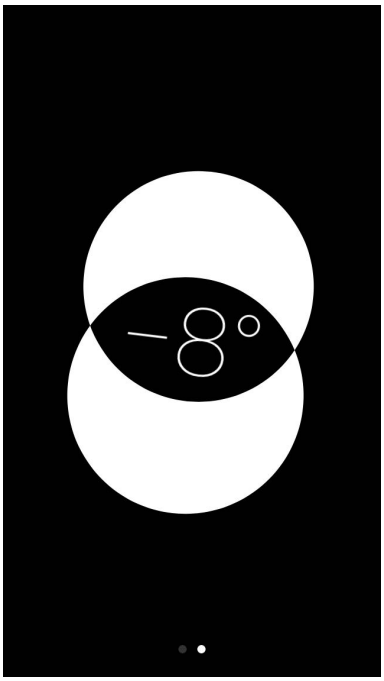

Figure 4.3: Native iOS application - Compass

4.3.2 Experiment Configuration

After deciding the preferred values of R matrix of the Kalman filter for the current hardware setup, comparison of complementary filter and Kalman filter was done in stationary and in-motion scenarios. The IMU had the facility to save all the output into a micro SD card. We utilized this provision with an in-motion scenario where the IMU was fixed on a toy-train and a serial connection to obtain the result was not possible. The roll and pitch values were captured while the train is not moving (stationary) and when the train is in motion. With the toy train experiment, the angles at which the experiment is performed are measured using a native iOS application application – "Compass". As shown in figure 4.2, this application gives us the different angles based on the position of iPhone along with its internal sensors. We are using an iPhone 5s as the device to obtain different roll and pitch angles. As per the technical specifications of the iPhone 5s released by Apple on 16th May 2018 [80], it contains a high quality three-axis gyroscope, accelerometer along with assisted GPS and GLONASS sensors. Hence, this model of iPhone must be able to give us accurate angles with the help of its native Compass application. The roll and

pitch angles obtained from the two filters were analyzed along with the time taken for each filter to reach the predefined angle.

4.3.3 Data Analysis Procedure

This section covers the data analysis procedure for the comparison of complementary and Kalman filter. As per our preliminary understanding the complimentary filter will be unable to completely eliminate the errors caused by drifts and noises in sensors [3]. Hence, the results obtained from Kalman filter was expected to be better than the complementary filter due its capability of identifying and eliminating the errors. The sensor data captured in all pre-defined positions was applied on the complementary filter and Kalman filter algorithm and the results obtained were compared along with baseline of raw value of accelerometer. The comparison were made as follows.

Overall, there were two scenarios in the experiments : Stationary and in-motion. Each of these scenarios had four different angles at which the experiments were performed : 15, 30, 45 and 60. These angles were selected just as an example to perform the experiments.

The IMU was mounted on a toy train similar to the R matrix sensitivity experiment. Stationary experiment was performed without the movement of toy train. In-motion experiment was performed by moving the toy train in a random track.

Scenario : Stationary / In-Motion

Predefined Roll/Pitch (angle)	Detected angle range by CF	Detected angle range by KF	Convergence time for CF (in seconds)	Convergence time for KF (in seconds)	SD of CF	SD of KF
15						
30						
45						
60						

Table 4.2: Comparison of complementary and Kalman filter

The result of these experiments were be displayed in the form of table 4.2, as

well as plotted as graphs using the tool - Matlab. Detected angle range explains the range of angles detected by the both filters after reaching the predefined angles in every experiment. The convergence time explains the time taken by both the complementary and Kalman filter to reach the predefined angles : 15, 30, 45 and 60 degrees. The standard deviation was calculated for all the pitch and roll angles to understand the stability of the filters. If the standard deviation is less, then the roll and pitch angles are more near to the predefined angle which can imply which filter is more precise to hold on to the converged angle.

With the help of these tables, we could identify the efficiency of Kalman filter algorithm over complementary filter algorithm in comparison to the raw sensor values.

Chapter 5

Experimental Results

The experimental results of both R matrix evaluation and the performance of complementary and Kalman filters are explained in the two sub-sections below. The first set of results is the analysis of the effect of sensor measurement error covariance matrix (R matrix) on the behaviour of Kalman filter. The R matrix is a 2X2 matrix which is initialized diagonally to help the Kalman filter matrix calculations [33]. The Kalman filter includes matrix transpose operation which imposes a major load on the processing load. Hence diagonal assignment of matrix values reduces this load as the transpose of a diagonal matrix is the same as the original matrix. The values chosen to tune R matrix is based on prior research work [33], [34], [35], [36] and the behaviour of the IMU used for the experiment. In total, a set of 5 values were short-listed to perform this experiment along with a predefined angle. Predefined angle is the baseline to understand the output of the Kalman filter. A comparison of all the results based on these 5 R matrix values were performed and a analysis was made towards convergence of roll and pitch angles of the aircraft to the predefined angle along with the measure of sensitivity of Kalman filter.

The second set of experiments validated the performance of complementary filter and Kalman filter on different roll and pitch angles. The Kalman filter experiment utilized the results of first research to gain an efficient precision of roll and pitch angles based on a set of R matrix values specific to the hardware setup used in this research. Finally a comparison of Kalman filter and complementary filter is performed to understand which filter produces high precision roll and pitch angles in both stationary and in-motion scenarios.

5.1 R Matrix Sensitivity Evaluation

The R matrix, being a 2X2 matrix, used five set of values to analyze the sensitivity on pitch and roll angles calculated using Kalman filter algorithm. Sections 5.1.1 and 5.2.1 covers these roll and pitch experiment results respectively and includes a comparison of the results to understand the effect of R matrix values. This result was utilized in obtaining a high-precision roll and pitch angles when applied on the Kalman filter algorithm, explained in the section 5.2

5.1.1 R Matrix Effect on Roll Experiment

This section covers the results of R matrix sensitivity experiment for roll angle calculation performed in the in-motion scenario. The results of these experiments are explained in the subsequent sections below. As explained in section 4.3.1, the five set of values were configured in the Kalman filter algorithm and the single set of raw gyroscope and raw accelerometer sensor measurements were utilized by Kalman filter algorithm calculate the pitch and roll angles.

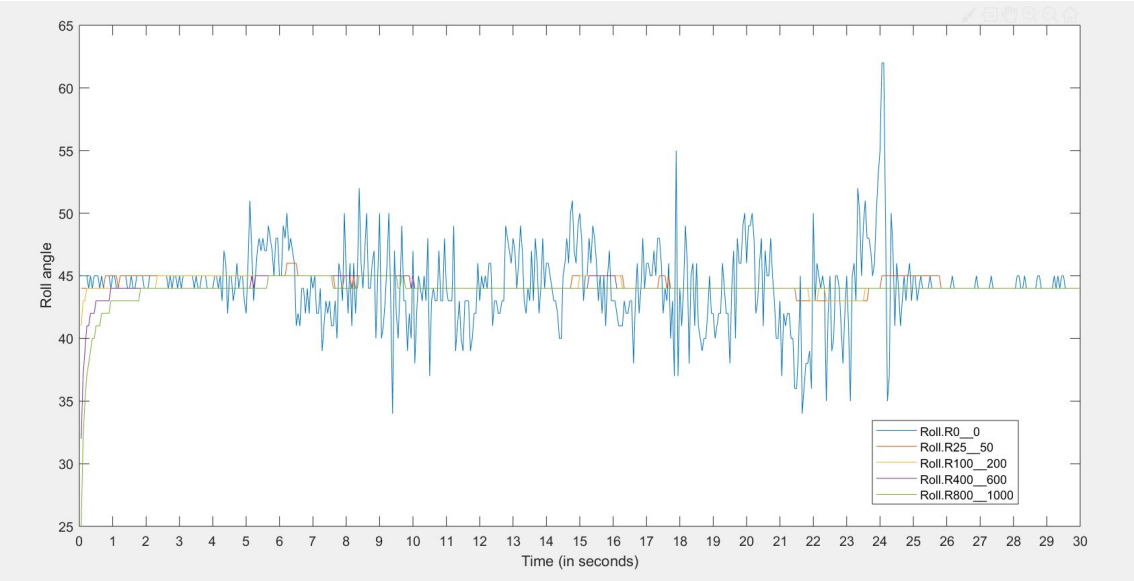

Figure 5.1: Roll angle experiment for R matrix sensitivity - 30 seconds

The in-motion roll experiment result is shown in the figure 5.1 above. We can clearly see that the first two values of R matrix, [0,0,0,0] and [25,0,0,50] help Kalman filter to reach the predefined angle of 45 degrees in less than a second. Third value

[100,0,0,200] takes around 2 seconds where as fourth value [400,0,0,600] and the final value [800,0,0,1000] of R matrix take around 5-6 seconds to reach 45 degrees. But, due to the severe vibrations created during the movement of toy train, the lower values of matrices shows higher sensitivity for Kalman filter algorithm results. This is visible in the graphs with severe variations of pitch and roll angles. The R matrix value - [0,0,0,0] makes Kalman filter highly sensitive and [25,0,0,50] improves the sensitivity by a smaller margin than previous case, but both are not satisfactory. The last three values of R matrix produces satisfactory results. The individual graphs of these results are shown in appendices section.

5.1.2 R Matrix Effect on Pitch Experiment

This section covers the results of R matrix sensitivity experiment for pitch angle calculation performed in the in-motion scenario. The values of R matrix are same as the roll experiment and the error and noise of the sensors also achieved in the same way.

The in-motion pitch experiment result is shown in the figure 5.2 below.

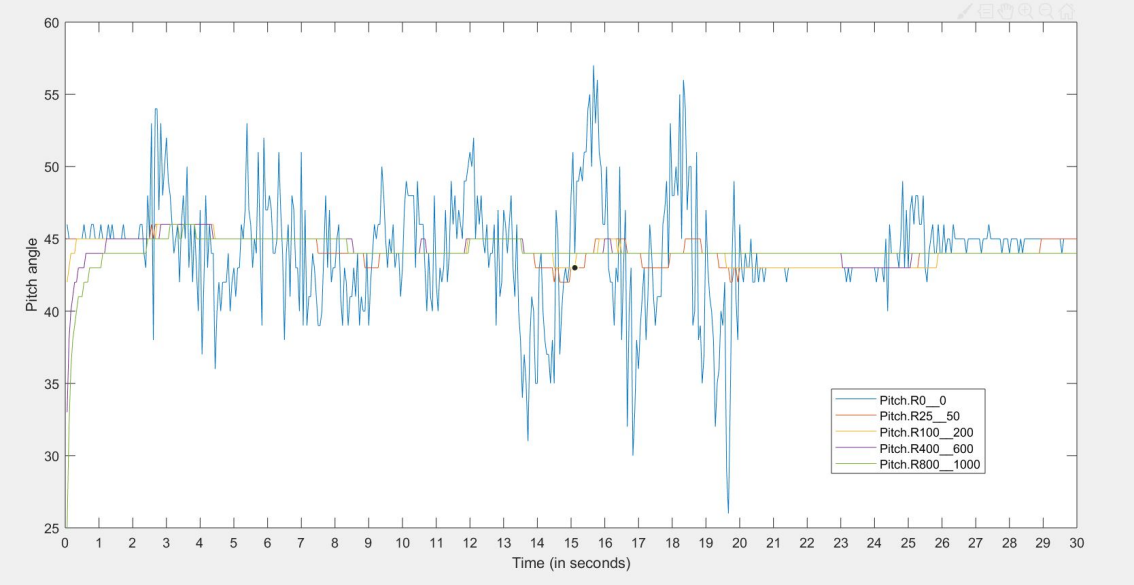

Figure 5.2: Pitch angle experiment for R matrix sensitivity - 30 seconds

The results of pitch angle calculation showed similar trends compared to the roll angle calculation experiment except the time taken by the Kalman filter executions

to reach predefined angle of 45 degrees was different. The first two values of the R matrix reach the predefined angle in less than a second. The third and fourth value of R matrix made Kalman filter reach the predefined angle around 2 seconds. Finally the Kalman filter achieved 45 degrees around 3 seconds with the final value of the R matrix.

5.1.3 Comparison and Analysis of R Matrix Sensitivity Results

This section summarizes all the results discussed in the above sections for R matrix sensitivity on Kalman filter algorithm and compares them with each other to measure the convergence time to the predefined angle of 45 degrees. The analysis of convergence time in seconds was made in addition to the sensitivity measure using the standard deviation of roll and pitch angle output by the Kalman filter.

5.1.3.1 Effect of R matrix values on the roll angle calculation

For the roll angle calculation, the Kalman filter execution results are summarized in the tables 5.1.

R matrix [2X2] values	Predefined angle x_i	Convergence time for Kalman filter (in seconds)	Standard Deviation $\sqrt{\frac{1}{N}\sum_{i=1}^{N}(x_i-\overline{x})^2}$
[0,0,0,0]	45	0.33	3.130
[25,0,0,50]	45	0.88	0.631
[100,0,0,200]	45	2.44	0.539
[400,0,0,600]	45	5.16	0.395
[800,0,0,1000]	45	5.67	0.362

Table 5.1: Results of R matrix effect on roll-angle-experiment

The convergence time of Kalman filter with the predefined angle increases as the R matrix values increase. When the R matrix values are completely eliminated by using the first set of values - [0,0,0,0], the convergence time is the least of 0.33 seconds to reach 45 degrees. As the R matrix values increase the convergence time increases to a maximum of 5.67 seconds with highest value that was tested in this research - [800,0,0,1000]. On the contrary, the standard deviation of the results decreases as R

matrix value increases. When the R matrix value is the least - [0,0,0,0], the standard deviation is 3.130. As the R matrix values increase, the standard deviation decreases. The highest R matrix value that was tested in this research - [800,0,0,1000] has the least standard deviation of 0.362 among all results of roll angle calculations.

5.1.3.2 Effect of R matrix values on the pitch angle calculation

For the pitch angle calculation, the Kalman filter execution results are summarized in the table 5.2.

R matrix [2X2] values	Predefined angle x_i	Convergence time for Kalman filter (in seconds)	Standard Deviation $\sqrt{\frac{1}{N}\sum_{i=1}^{N}(x_i - \overline{x})^2}$
[0,0,0,0]	45	0.05	3.915
[25,0,0,50]	45	0.05	0.950
[100,0,0,200]	45	1.27	0.853
[400,0,0,600]	45	1.33	0.681
[800,0,0,1000]	45	2.50	0.502

Table 5.2: Results of R matrix effect on pitch-angle-experiment

It is evident from the table that the R matrix effect on pitch angle calculation of Kalman filter is similar to that of the roll angle calculation explained in the previous section. The smallest value of R matrix makes the Kalman filter converge to the predefined angle in less than a second. As the R matrix values increase, the convergence time of Kalman filter with the predefined angle also increase. The largest R matrix values tested in this research - [800,0,0,1000] made the Kalman filter reach 45 degrees at 2.50 seconds. Standard deviation calculation of the R matrix effect in the pitch experiment showed similar results to the R matrix effect in the roll angle experiment. As the R matrix values increased, the standard deviation of pitch angle calculated by Kalman filter decreased. The least R matrix value - [0,0,0,0] showed the Kalman filter output of pitch angle had a standard deviation of 3.915. The highest R matrix value - [800,0,0,1000] had the lowest standard deviation of 0.502.

5.1.4 Summary

The graphs and the tables displaying the results of all the experiments were used to analyze the effect of R matrix on pitch and roll angle calculations using the Kalman filter. As the results indicated, the R matrix values play a major role in both convergence time and sensitivity of the Kalman filter algorithm. As the R matrix value increases, the sensitivity of Kalman filter decreases and the convergence time increases. This happens because, when the R matrix values increase, the Kalman filter gives higher precedence to previously calculated values than the newly calculated value [3]. When the previously calculated values are given higher precedence, the output from Kalman filter changes very slowly as indicated in the graphs. This results in a stable output from Kalman filter but a slower convergence to an actual angle of an object. On the other hand, smaller values of R matrix makes Kalman filter to give a higher precedence to the latest calculated roll and pitch angles than the previously calculated values. This results in quick update of roll and pitch angle of an object, but the errors and noise would not get completely eliminated. Hence, there is a faster convergence but the output of roll and pitch angles are more prone to errors. This happens because, when a high value of R matrix is configured, it makes the Kalman filter to trust the previously measured values more than the new sensor measurements [33]. Hence, new measurements that might be showing a change in angle is reflected slowly as the Kalman filter relies on previous angle calculated by itself. On the other hand, if a small value is configured for R matrix, it trusts the sensor measurements more than the previously calculated value. So, the output measured by the Kalman filter is quick to reflect the change in angle as the sensor updates it. This results in Kalman filter being very sensitive to the vibrations. For instance, from the results, [Appendix A] it is evident that when the R matrix is completely eliminated by configuring zeros, the sensitivity of Kalman filter is so high that it is completely unusable.

To summarize the results, whenever a Kalman filter is used to calculate roll and pitch angle of an object, the R matrix has to be chosen wisely based on the type of sensors as well as the hardware setup used in the experiment. When R matrix

values are small, the convergence time is fast but the Kalman filter becomes very sensitive. As the R matrix values increase, the convergence time becomes slow but the Kalman filter becomes stable. Hence, there is a trade-off while choosing the R matrix value. If a fast behaviour of filter is the main requirement, then a smaller R matrix values can be chosen but there is a compromise on the stability of the filter. If a stability of the filter is the main requirement, then larger R matrix values can be chosen compromising on the convergence time of Kalman filter.

5.2 Performance of Complementary and Kalman Filter Based Schemes

The second part of research was to compare and analyze the performance of complementary filter and Kalman filter algorithms while calculating the roll and pitch angles. Both the pitch and roll angle measurements were calculated for two scenarios : stationary and in-motion with 4 different angles. The raw accelerometer and raw gyroscope values were considered as the baseline to understand the performance of these filters. The same hardware setup used in the first experiment of R matrix sensitivity was used in this part of experiment. To measure the four different angles, the iPhone 5s was used similar to first experiment. In total, we gathered 16 different results from all these experiments and compared the results to understand which filter performs better. The roll angle experiment results are presented in section 5.2.1, followed by the pitch angle experiment results in section 5.2.2 respectively, for both stationary and in-motion scenarios with 4 different predefined angles. In-motion experiments are performed using a toy-train to achieve the noise created due to vibrations in the movement.

5.2.1 Roll Angle Calculations

Stationary scenario for roll angle calculation covers the four angles : 15, 30, 45 and 60. Raw values of accelerometer and gyroscope sensors are considered as the baseline along with the predefined angle captured using iPhone 5s, and the complementary filter along with the Kalman filter results are plotted using Matlab graphs. Each image shows the pre-defined angle set for the experiment and time taken by both the filters to reach that angle. The results of first 30 seconds from the experiment are

shown below in both stationary and in-motion scenarios.

5.2.1.1 Stationary scenario

The stationary roll experiment result for the predefined angle of 15 degrees is shown in the figure 5.3 below.

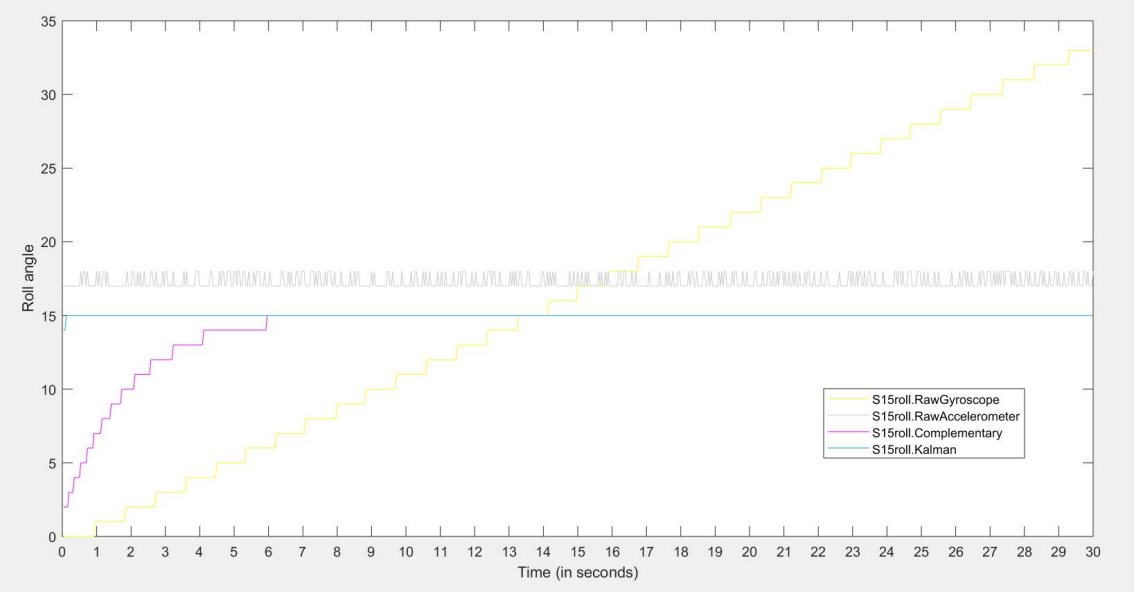

Figure 5.3: Stationary-roll experiment for 15 degrees

It can be seen from the figure that accelerometer and Kalman filter took less than a second (0.11 seconds) to reach the predefined angle of 15 degrees. But, the complementary filter was very slow in reaching the predefined angle of 15 degrees. It took almost 5.96 seconds to reach 15 degrees even though it reached 14 degrees in about 4 seconds. Raw accelerometer sensor readings had severe noise and errors which made it almost reach 17 to 18 degrees. Raw gyroscope sensor readings showed the rate of change of angle in every timeslot, hence could not be compared with these three results.

The stationary roll experiment result for predefined angle of 30 degrees is shown in the figure 5.4 below. As the graph indicated, the accelerometer was the fastest to reach predefined angle of 30 degrees. Once again, the Kalman filter took less than one second (0.19 seconds) to reach roll angle of 30 degrees. Similar to the results from previous experiment, the complementary filter was slow and took 7.38 seconds to

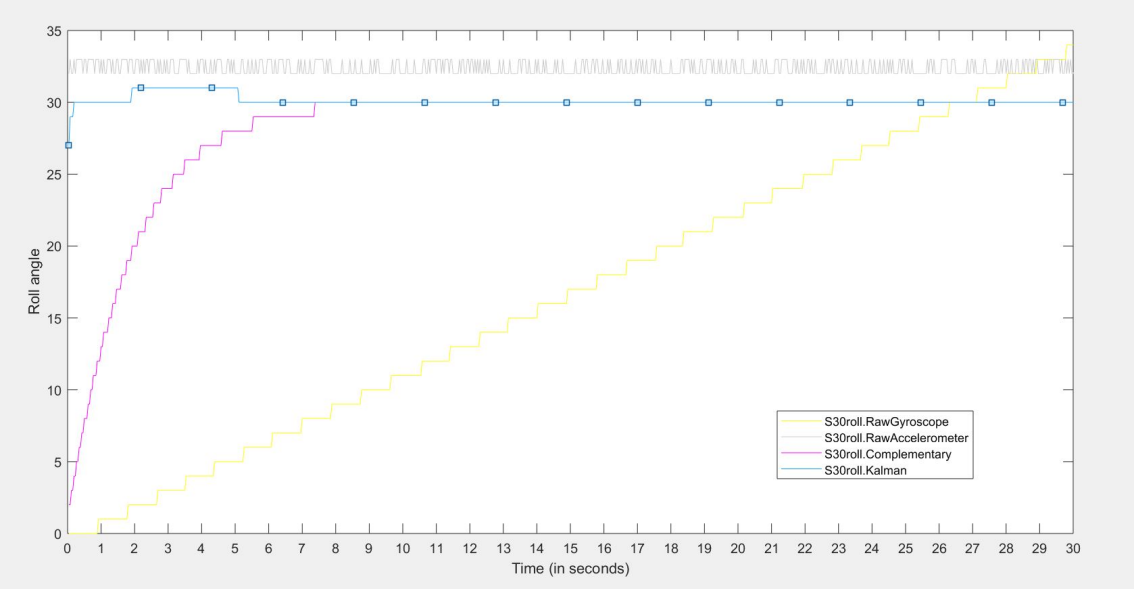

Figure 5.4: Stationary-roll experiment for 30 degrees

reach 30 degrees. Due to the errors in Raw accelerometer sensor readings, it hovered between 32 to 33 degrees. Raw gyroscope sensor readings showed the rate of change of angle in every timeslot, hence could not be compared with these three results.

The stationary roll experiment result for predefined angle of 45 degrees is shown in the figure 5.5 below. The accelerometer sensor reached 45 degrees in no time,

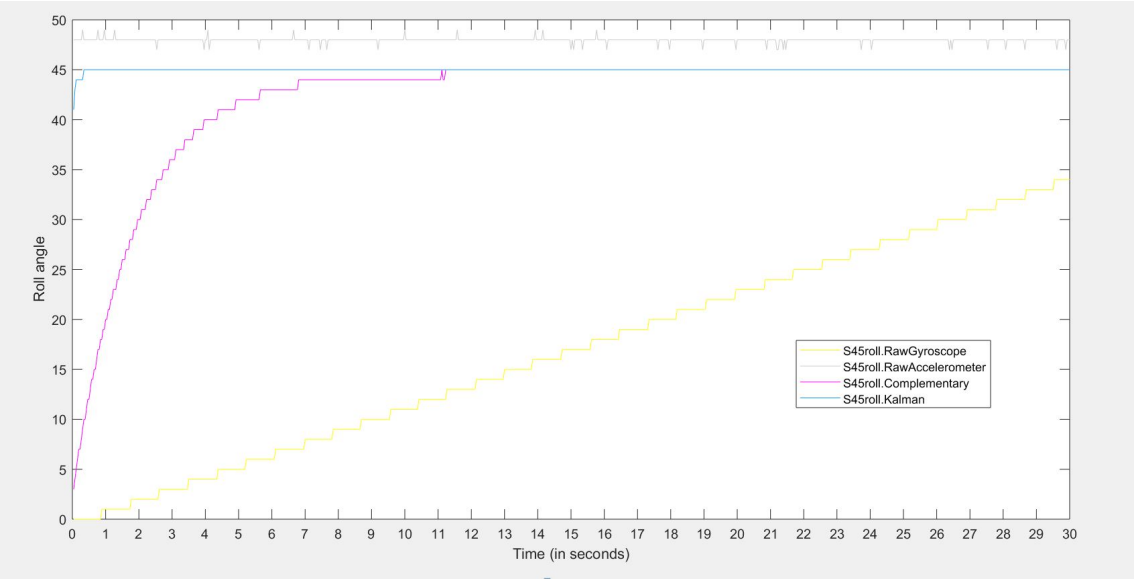

Figure 5.5: Stationary-roll experiment for 45 degrees

but suffered from errors even in stationary scenario. The Kalman filter once again took less than one second (0.34 seconds) to reach the predefined angle of 45 degrees. In this case, the complementary filter took 11.11 seconds to reach 45 degrees, even though it reached 44 degrees in 6.84 seconds. The last change of 1 degree took about 5 seconds which shows that the performance of complementary filter was very slow. Raw gyroscope sensor readings showed the rate of change of angle in every timeslot, hence the results were not compared with roll angle output from the filters.

The stationary roll experiment result for the predefined angle of 60 degrees is shown in the figure 5.6 below. Once again the accelerometer was the fastest to reach

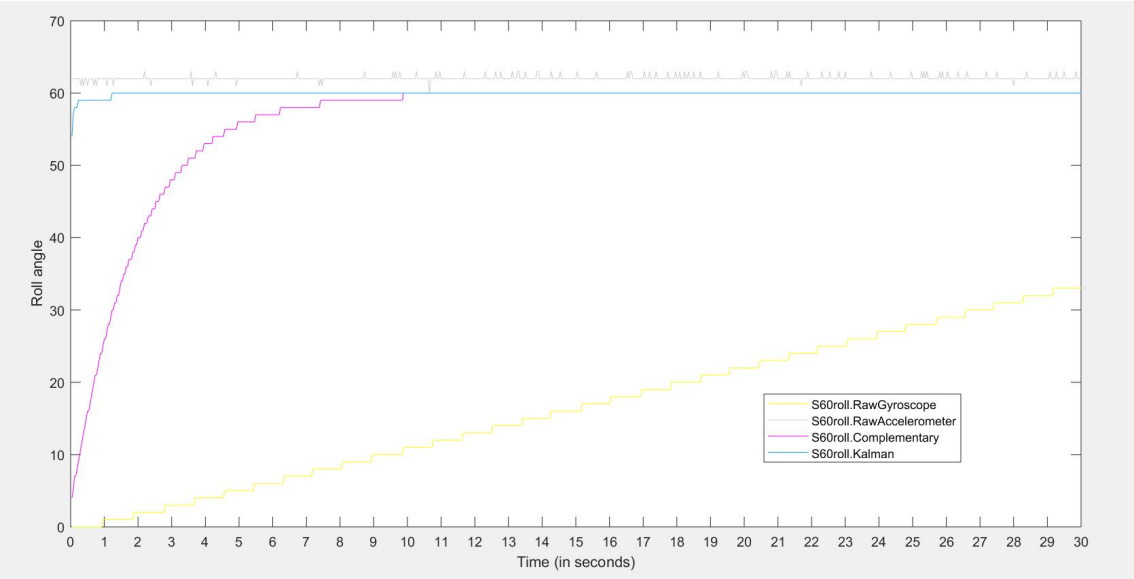

Figure 5.6: Stationary-roll experiment for 60 degrees

60 degrees but it was affected with errors which made it to reach almost 63 degrees occasionally. The Kalman filter took 1.23 seconds to reach the predefined angle of 60 degrees whereas the complementary filter took 9.88 seconds to reach the same. Similar to the previous case, even though complementary filter reached 59 degrees in 7.53 seconds, the convergence into the last one degree took around 2.43 seconds. Similar to previous results, the raw gyroscope sensor readings were not compared with the roll angle output from the filters.

The table describing overall results from stationary scenario for all the tested

predefined roll angles is shown below.

Predefined Roll (angle)	Detected angle range by CF	Detected angle range by KF	Convergence time for CF (in seconds)	Convergence time for KF (in seconds)	SD of CF	SD of KF
15	15	15	5.96	0.11	2.263	0.050
30	30-31	30	7.38	0.19	4.791	0.334
45	44-45	45	11.11	0.34	0.228	0.182
60	60	60	9.88	1.23	9.519	0.322

Table 5.3: Comparison of complementary and Kalman filter for roll angle calculation. Scenario : Stationary

Due to the errors in accelerometer sensor along with the gyroscope sensor providing the change of rate of angle, they were not included in the performance analysis, hence they were not a part of the table. Detected angle range of complementary filter had a slight deviation to the predefined angle by one degree, even though the experiment was a stationary scenario, indicating there was no movement. The detected angle range of Kalman filter was very consistent to the predefined angle. The convergence time for the Kalman filter was far superior compared to the convergence time of the complementary filter. The standard deviation of both the filters in each case also indicated the Kalman filter was the faster as well as more stable after reaching the predefined angle compared to the complementary filter. This shows that the Kalman filter is a more efficient algorithm compared to the complementary filter for roll angle calculation in stationary scenario.

5.2.1.2 In-motion scenario

This section shows the results of roll angle experiment in the in-motion scenario. The movement was achieved by fixing the hardware(IMU) on a toy train in different angles such as 15, 30, 45 and 60 degrees.

The in-motion roll experiment result for predefined angle of 15 degrees is shown in the figure 5.7 below. As it is seen in the figure, accelerometer and Kalman filter

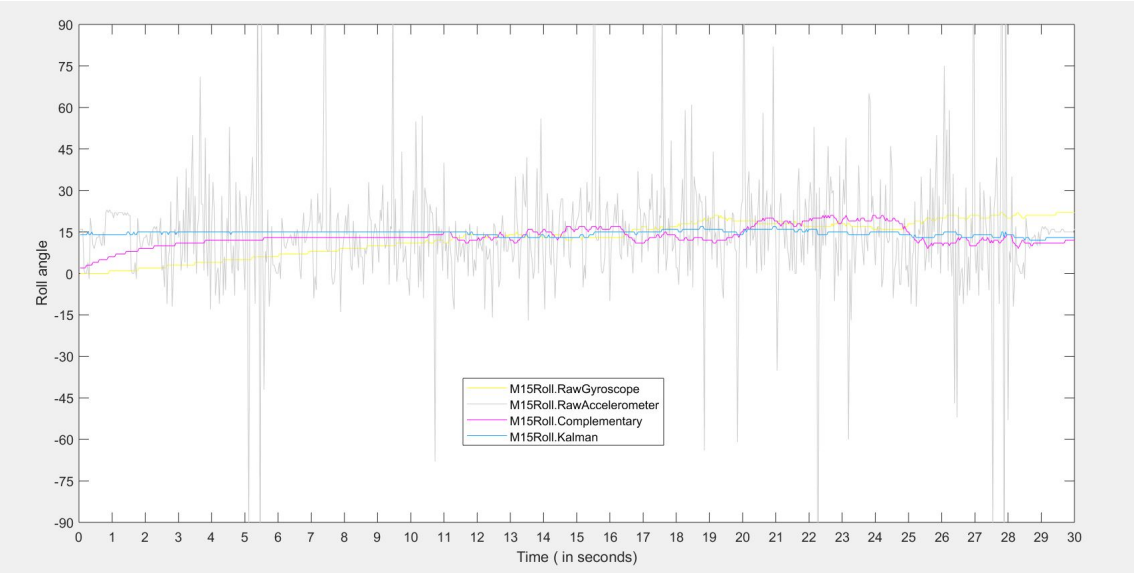

Figure 5.7: In motion-roll experiment for 15 degrees

reached the predefined angle very fast compared to the complementary filter. Accelerometer reached 15 degrees faster than the Kalman filter, but it showed severe errors due to the movement of the toy train (shown in grey color). Kalman filter took 0.26 seconds to reach the predefined angle and it was pretty consistent around 15 degrees. Complementary filter took 11 seconds to to reach the same which was very slow convergence. Also, the variations in roll angles calculated by complementary filter was (shown in pink color) higher than variations calculated by Kalman filter (shown in blue color). Raw gyroscope sensor readings showed the rate of change of angle in every timeslot, hence could not be compared with the performance of filters.

The in-motion roll experiment result for predefined angle of 30 degrees is shown in the figure 5.8 below. Accelerometer sensor once again took the least amount of time to reach predefined angle of 30 degrees, but due to the errors created during the movement the roll angle was very inconsistent as there are huge deflections in the graph (shown in grey color). The Kalman filter took only 0.19 seconds to reach 30 degrees and it was very consistent with minor variations (shown in blue color). The complementary filter took about 11.34 seconds to reach 30 degrees, whereas it had reached 28 degrees within 5.53 seconds itself. The final convergence of 2 degrees took almost 6 seconds indicating poor performance of complementary filter. Also, the

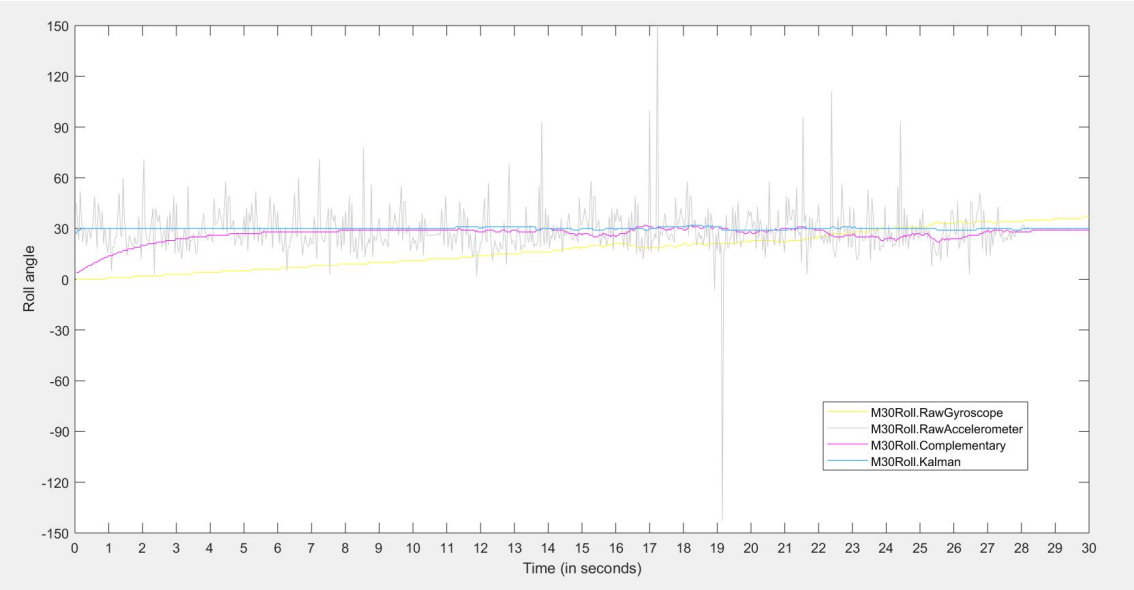

Figure 5.8: In motion-roll experiment for 30 degrees

variations after reaching predefined angle is higher for complementary filter (shown in pink color) compared to the Kalman filter. Raw gyroscope sensor readings were once again ignored in the comparison analysis due to the similar reasons as described above.

The in-motion roll experiment result for predefined angle of 45 degrees is shown in the figure 5.9 below. Similar to all previous experiments, the accelerometer sensor was the fastest to converge into 45 degrees, but showed severe errors due to the movement (shown in grey color). The Kalman filter took only 0.34 seconds to reach the predefined angle of 45 degrees, whereas the complementary filter took about 5.31 seconds to reach the same. Even though complementary filter was faster in converging to 45 degrees compared to previous two cases of 15 and 30 degrees of roll experiment (figures 5.7 and 5.8), it was definitely not faster than the Kalman filter. Also, the errors caused by the movement of toy train was not completely eliminated by the complementary filter in comparison to the Kalman filter. This can seen by the output of complementary filter (in pink color) varying over time compared to the Kalman filter output (in blue color).

The in-motion roll experiment result for predefined angle of 60 degrees is shown

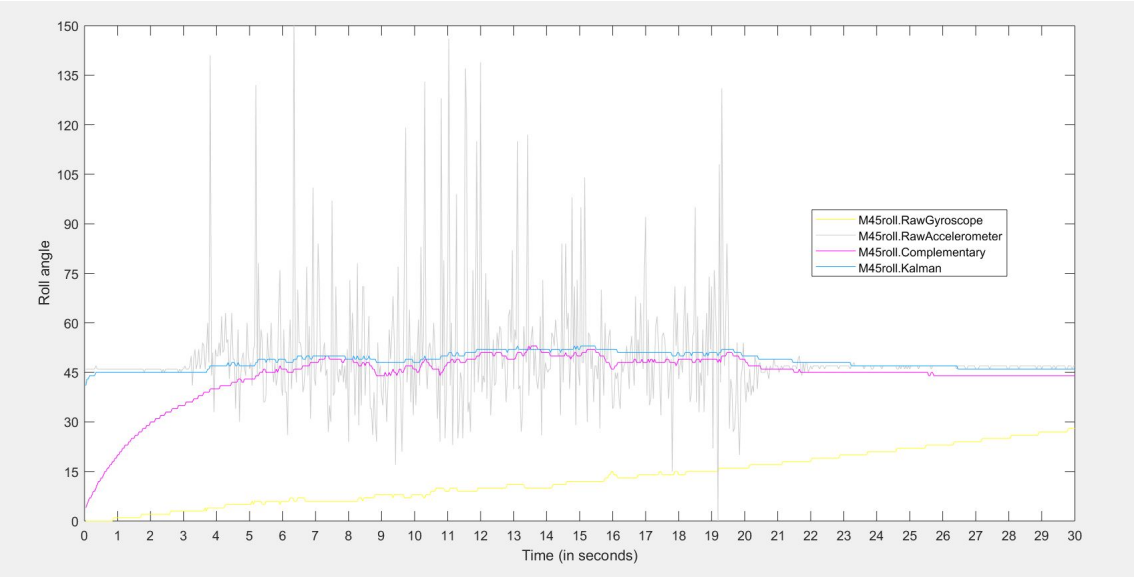

Figure 5.9: In motion-roll experiment for 45 degrees

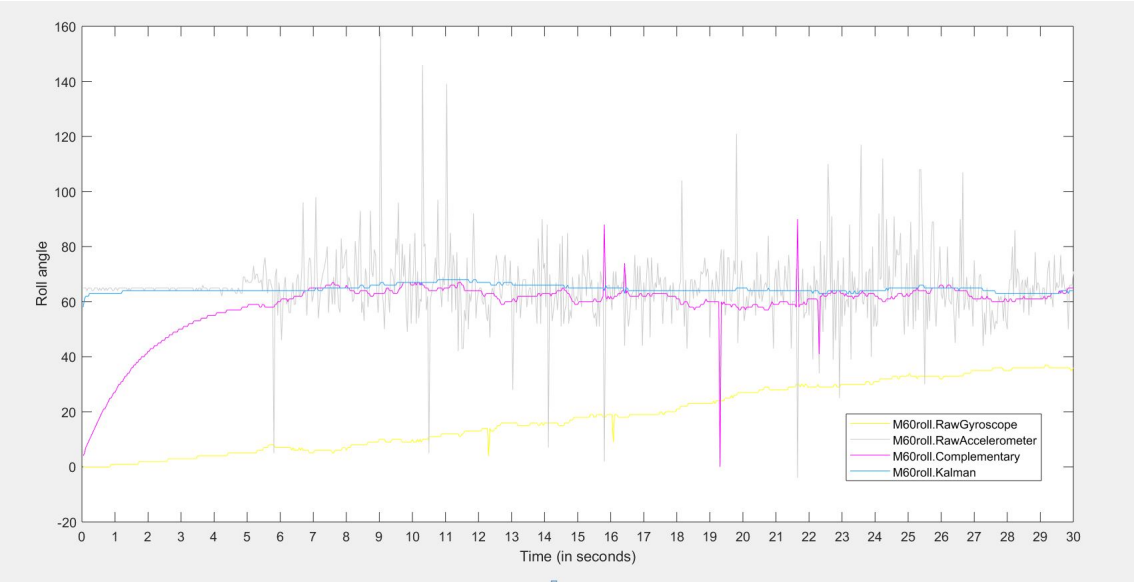

Figure 5.10: In motion-roll experiment for 60 degrees

in the figure 5.10 above. It can be seen from the figure that the accelerometer showed the similar behaviour as the previous experiments. It was very fast and easily prone to errors due to the movement of toy train, hence very unstable (shown in grey color). The Kalman filter took only 0.7 seconds to reach the predefined angle of 60 degrees which was way faster than the complementary filter which took 5.92 seconds to reach the same. Similar to the previous experiment, the complementary filter couldn't

completely eliminate the errors during the roll angle calculation, hence there are few severe deflections (shown in pink color). Kalman filter has some minor variations (shown in blue color) around 45 degrees, but the performance is better than complementary filter. Raw gyroscope sensor readings showed the rate of change of angle in every timeslot, hence they were not included in the analysis.

The table describing overall results from in-motion scenario for all the tested predefined roll angles is shown below. Once again, the severe errors in raw accelerometer

Predefined Roll (angle)	Detected angle range by CF	Detected angle range by KF	Convergence time for CF (in seconds)	Convergence time for KF (in seconds)	SD of CF	SD of KF
15	9-21	12-17	11	0.26	3.474	0.980
30	22-32	29-32	11.34	0.19	4.417	0.611
45	44-53	45-53	5.31	0.34	7.948	2.406
60	-5 to 92	58-65	5.92	0.07	10.308	1.281

Table 5.4: Comparison of complementary and Kalman filter for roll angle calculation. Scenario : In-motion

sensor data due to the movement of toy train along with raw gyroscope sensor data showing only rate of change of angle, they were not included in the table as well as analysis of filters. As shown in second and third column of the table, the detected angle range of the complementary filter varied a lot compared to the range of angle captured the by Kalman filter. For example, in case of 30 degrees of roll angle, the complementary filter ouput varied between 22 to 32 degrees after reaching 30 degrees. Also, when the predefined angle was 60 degrees, the detected angle range of the complementary filter was between -5 to 92 degrees, which was very huge. The detected angle range by the Kalman filter is less than 5 degrees in every case. Also the standard deviation calculated for Kalman filter showed lower values compared to the complementary filter in all experiments. This proved that the Kalman filter could eliminate the errors more efficiently compared to the complementary filter.

5.2.2 Pitch Angle Calculations

Similar to the evaluation of the complementary and the Kalman filter for roll angle experiment, a set of experiments were performed for calculating pitch angles with the model aircraft in the same four predefined angles : 15, 30, 45 and 60. The results of these experiments are shown in below sections.

5.2.2.1 Stationary scenario

The stationary pitch experiment result for predefined angle of 15 degrees is shown in the figure 5.11 below. It can be seen from the figure that the accelerometer sensor

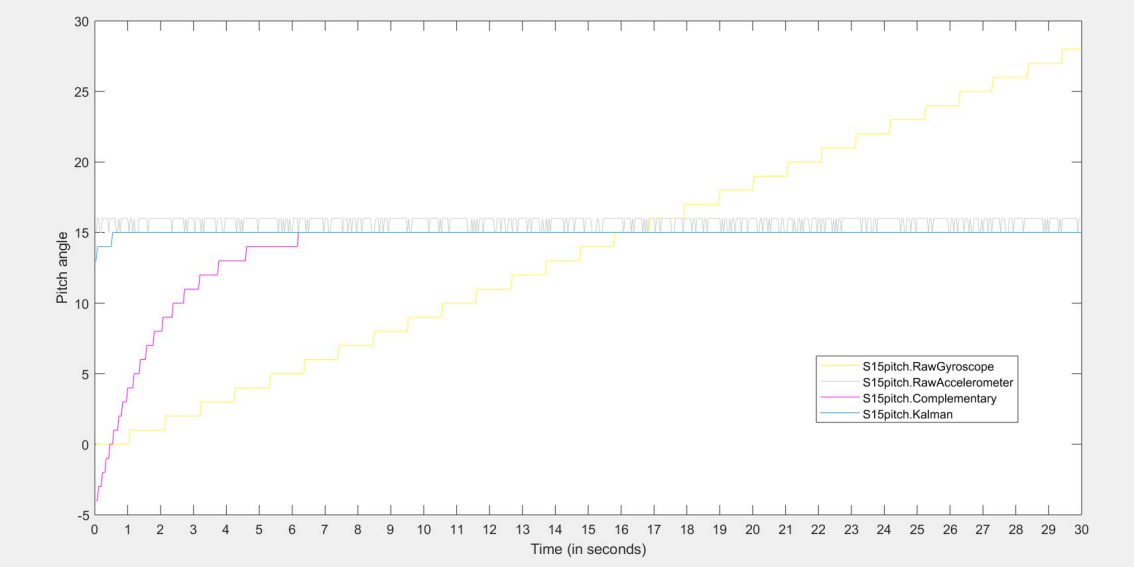

Figure 5.11: Stationary-pitch experiment 15 degrees

was the fastest among all to reach 15 degrees, but it clearly showed small errors even in stationary scenario (shown in grey color). The Kalman filter took 0.53 seconds to reach the predefined angle of 15 degrees and it is very stable after reaching it. Complementary filter took 6.23 seconds to reach the 15 degrees and the convergence of last one degree took 1.33 seconds. After reaching the predefined angle, the complementary filter was also stable similar to Kalman filter and held onto 15 degrees, as there were no movement of toy train in the stationary scenario. Raw gyroscope sensor readings were ignored as they did not show the actual roll angle.

The stationary pitch experiment result for predefined angle of 30 degrees is shown

in the figure 5.12 below Similar to previous results, the accelerometer was the fastest

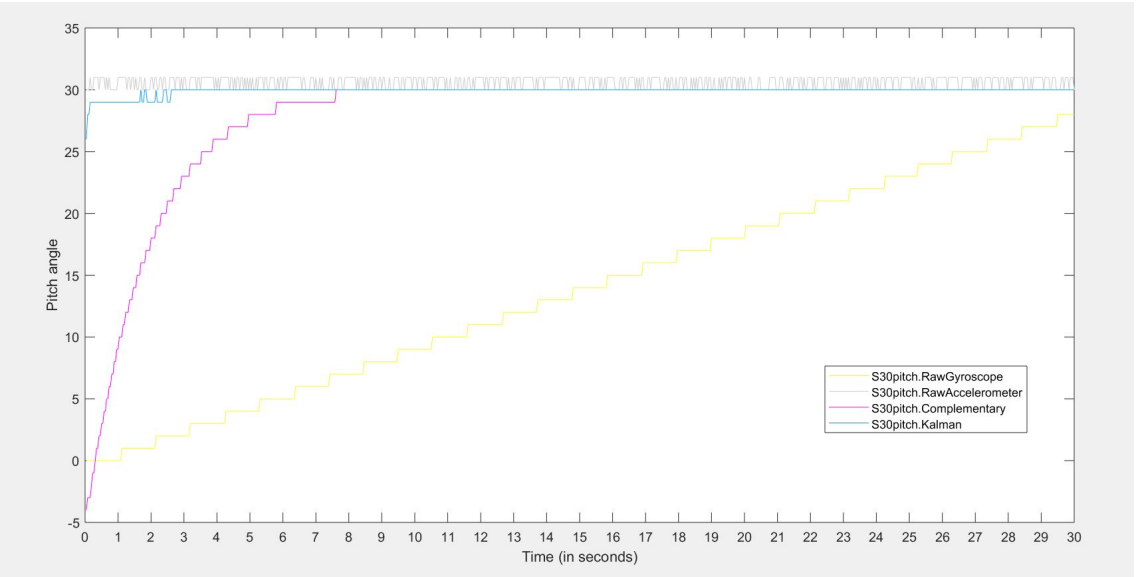

Figure 5.12: Stationary-pitch experiment 30 degrees

but suffered from errors even in stationary scenario (shown in grey color). The Kalman filter took 1.81 seconds to reach the predefined angle of 30 degrees. The complementary filter took 7.57 seconds to reach the same. Both the complementary filter as well as the Kalman filter did not suffer from any errors after reaching 30 degrees and held on to it. Raw gyroscope sensor readings were ignored for the same reasons as explained in previous result sections.

The stationary pitch experiment result for predefined angle of 45 degrees is shown in the figure 5.13 above. It can be seen from the figure that accelerometer being the fastest to reach 45 degrees suffered from minor errors. It was very unstable even in stationary scenario (shown in grey color). The Kalman filter took 0.23 seconds to reach the predefined angle whereas the complementary filter took 6.76 seconds to reach the same. Also, it can be seen that after 8.73 seconds, the detected angle of the complementary filter showed the pitch angle as 16 degrees which is actually more than predefined angle. The Kalman filter stayed at 15 degrees throughout the duration of the test. Raw gyroscope sensor readings were ignored for stand alone analysis due to the similar reasons explained in above result sections.

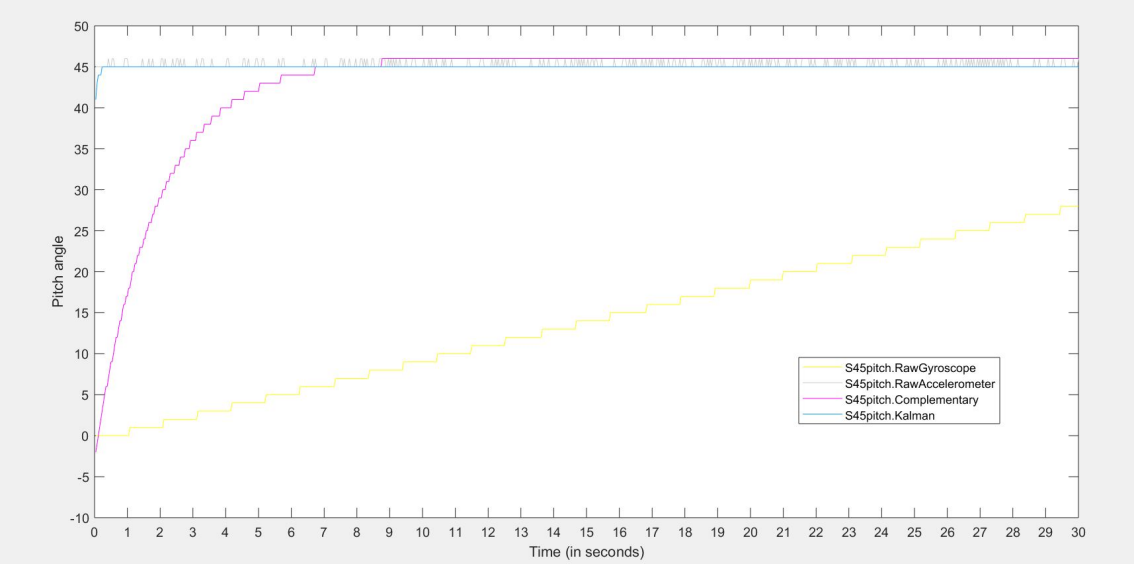

Figure 5.13: Stationary-pitch experiment 45 degrees

The stationary pitch experiment result for predefined angle of 60 degrees is shown in the figure 5.14 below. As seen from the figure, the accelerometer was once again

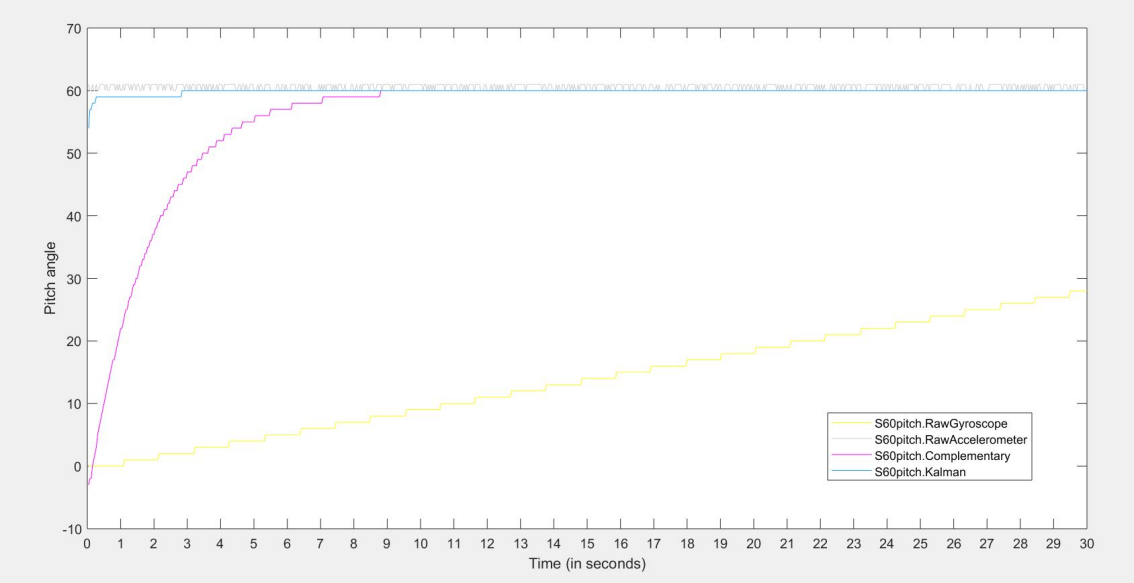

Figure 5.14: Stationary-pitch experiment 60 degrees

highly unstable (shown in grey color) throughout the duration of testing even though it was faster than all other filters. The Kalman filter took 2.88 seconds to reach the predefined angle of 60 degrees which was higher than its performance in the

previous three experiments with pitch angles - 15, 30 and 45. The complementary filter took 8.73 seconds to reach the same. Once again, both the filters did not show any variations after reaching the predefined angle. But the complementary filter was very slow compared to the Kalman filter in the convergence time to the predefined angle.

The table 5.5 describes overall results from stationary scenario for all the tested predefined pitch angles. Similar to the previous experiments, the raw accelerometer sensor data and the raw gyroscope sensor data were not included in the table as well as analysis of filters. In this set of experiment, the detected angle range of

Predefined Pitch (angle)	Detected angle range by CF	Detected angle range by KF	Convergence time for CF (in seconds)	Convergence time for KF (in seconds)	SD of CF	SD of KF
15	15	15	6.23	0.53	3.213	0.142
30	30	28-30	7.57	1.81	5.820	0.311
45	45-47	45	6.76	0.23	8.013	0.171
60	60	60	8.73	2.84	10.725	0.398

Table 5.5: Comparison of complementary and Kalman filter. Scenario : Stationary

the complementary filter as well as the Kalman filter did not suffer huge variations, as expected, due to the stationary behaviour of the scenario tested. But, the time taken by complementary filter was significantly more than Kalman filter to reach the predefined angles. Also the lower values of the standard deviation calculated for Kalman filter proved a higher convergence rate as well as the stability of Kalman filter compared to the complementary filter for all predefined angles. This proved that the Kalman filter can eliminate the errors more efficiently compared to the complementary filter for pitch angle calculation in stationary scenario.

5.2.2.2 In-motion scenario

This section shows the results of pitch angle experiment in the in-motion scenario. Similar to the roll angle experiments, the movement was achieved by fixing the hardware(IMU) on a toy train in different angles such as 15, 30, 45 and 60 degrees.

The in-motion pitch experiment result for predefined angle of 15 degrees is shown in the figure 5.15 below. It can be seen from the figure that the accelerometer sensor

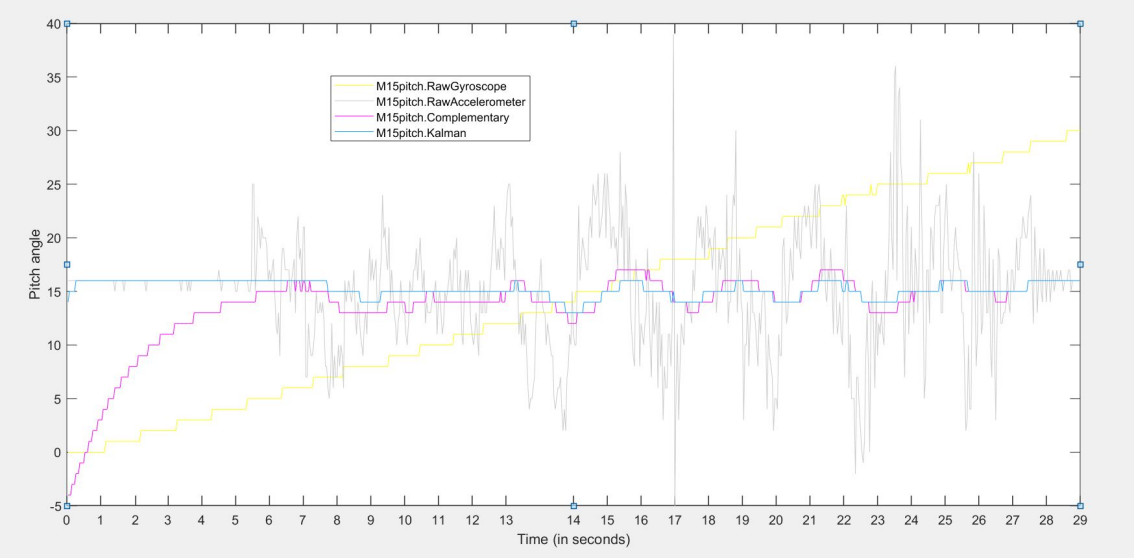

Figure 5.15: In motion-pitch experiment 15 degrees

readings were highly unstable as it suffered from the errors created due to the movement with the in-motion scenario (shown in grey color). The Kalman filter being the fastest took only 0.07 seconds to reach the predefined angle of 15 degrees. It suffered from minor errors (shown in blue color), but the error of angle range of Kalman filter was less than 3 degrees to its predefined angle. Complementary filter took 5.61 seconds to reach the angle of 15 degrees, but even this filter suffered from errors (shown in pink color) which were higher than the Kalman filter. The raw gyroscope sensor readings showed the rate of change of angle in every timeslot, hence could not be compared with these three results.

The in-motion pitch experiment result for predefined angle of 30 degrees is shown in the figure 5.16 below. Once again the accelerometer sensor suffered from severe errors during movement (shown in grey color). The Kalman filter took only 0.61 seconds to reach the predefined angle of 30 degrees. Also, it was clearly evident from the graph that Kalman filter was very consistent to the predefined angle (shown in blue color) and eliminated most of the errors. The complementary filter took 3 seconds to reach 30 degrees which was faster than the time it took to reach 15

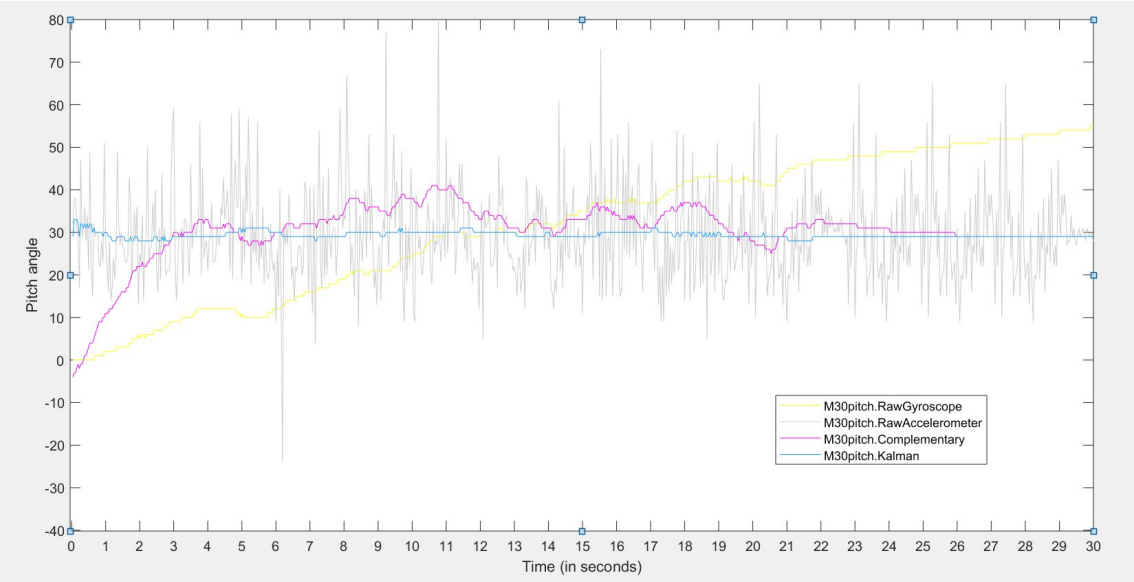

Figure 5.16: In motion-pitch experiment 30 degrees

degrees in previous experiment. But the complementary filter showed a higher error rate (shown in pink color) as it almost reached near to 40 degrees around 11.11 seconds. Raw gyroscope sensor readings were ignored for the analysis of filters due to its behaviour of showing the rate of change in angle.

The in-motion pitch experiment result for predefined angle of 45 degrees is shown in the figure 5.17 below. It can be seen from the figure that the accelerometer sensor suffered from errors due to the noise captured during the movement (shown in grey color). The Kalman filter took only 0.07 seconds to reach the predefined angle of 45 degrees which is very fast and it maintained its detected angle range within a small range of 3 degrees to prove its stability (shown in blue color). On the other hand, the complementary filter took 4.61 seconds to reach 45 degrees. Also, the pitch angle range detected by complementary filter varied a lot, sometimes reaching as low as -4 degrees (shown in pink color). Raw gyroscope sensor readings show the rate of change of angle in every timeslot, hence could not be compared with these three results.

The in-motion pitch experiment result for predefined angle of 60 degrees is shown in the figure 5.18 below. It can be seen from the figure that the accelerometer sensor suffered from errors due to the movement which made it very unstable throughout

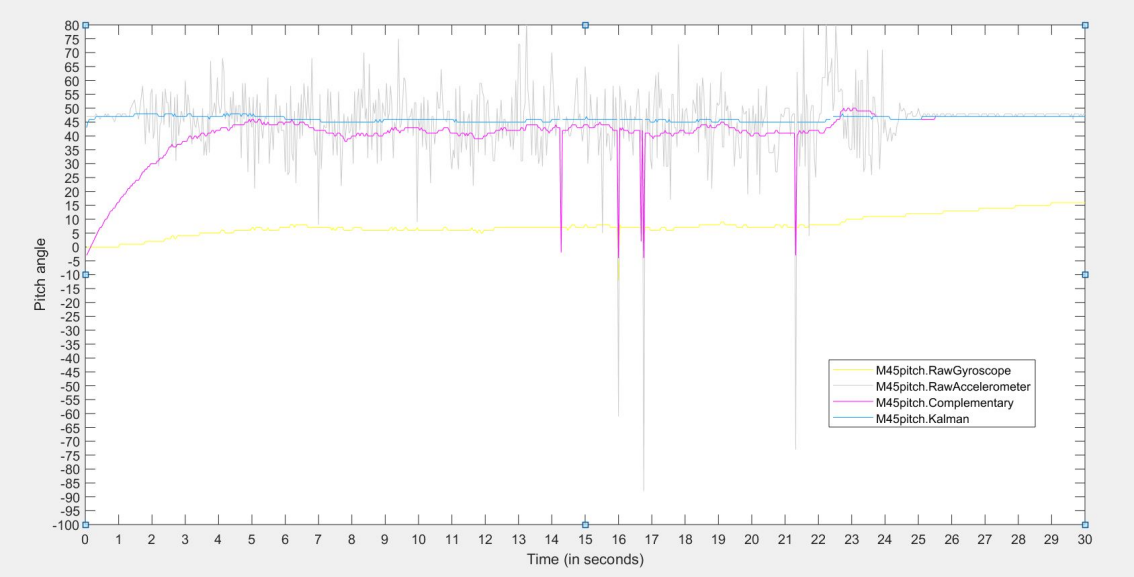

Figure 5.17: In motion-pitch experiment 45 degrees

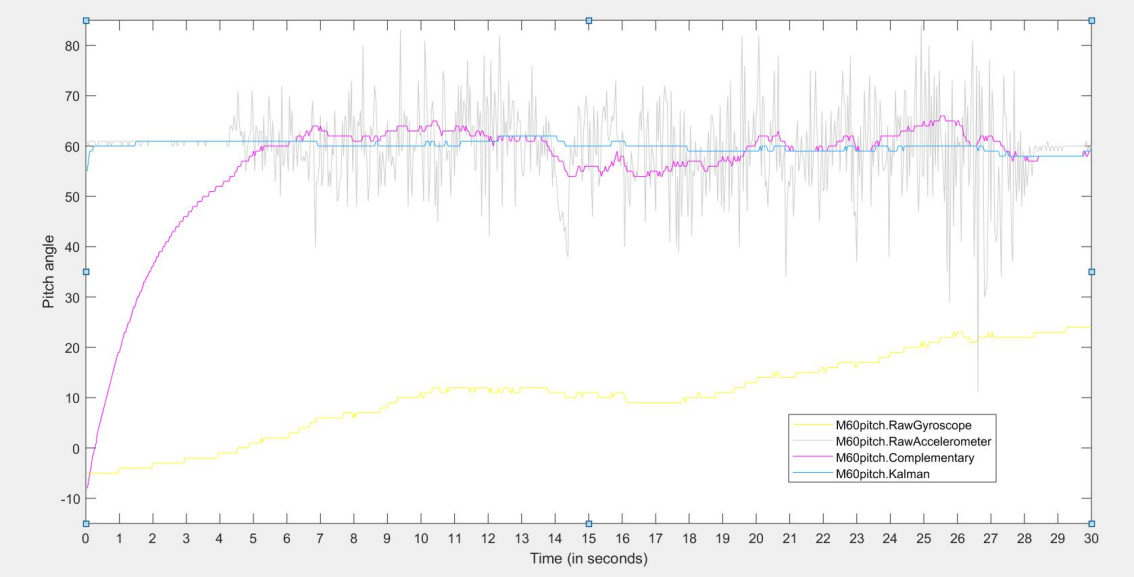

Figure 5.18: In motion-pitch experiment 60 degrees

the experiment. The Kalman filter took only 0.23 seconds to reach the predefined angle of 60 degrees and it maintains its angle range within 2 degrees by eliminating all the errors (shown in blue color). The complementary filter takes 4.65 seconds to reach the angle of 60 degrees and the angle range hovered between 54 degrees to 65 degrees due to the incomplete error and noise elimination(shown in pink color). Raw gyroscope sensor readings were once again ignored for the analysis of the filters.

The table describing overall results from in-motion scenario for all the tested predefined angles is shown below. As seen in the table, the convergnce time to the

Predefined Pitch (angle)	Detected angle range by CF	Detected angle range by KF	Convergence time for CF (in seconds)	Convergence time for KF (in seconds)	SD of CF	SD of KF
15	12-17	13-16	5.61	0.07	3.400	0.753
30	25-41	28-33	3	0.61	6.699	0.758
45	-4-50	43-48	4.61	0.07	8.561	0.916
60	54-65	60-62	4.65	0.23	11.717	1.029

Table 5.6: Comparison of complementary and Kalman filter. Scenario : In-motion

predefined pitch angle of 60 degrees was significantly high for the complementary filter compared to the Kalman filter in all cases. The complementary filter had the convergence time between 3 to 6 seconds based on the predefined angle, where as all the convergence time of the Kalman filter were less than one second. Also, the detected angle range of the complementary filter was much higher than Kalman filter which explained the stability of the Kalman filter as more precisive than the complementary filter. The standard deviation calculation of all the predefined angles also explain the same. The distribution of detected angle range is very close to the mean for a Kalman filter than a complementary filter. Hence, the observation from in-motion scenario of pitch angle experiment was that the Kalman filter could eliminate the errors more efficiently than the complementary filter and also, the Kalman filter is faster in converging to the predefined angles.

5.2.3 Memory Utilization

The experimental platform had a low powered processor and limited memory as explained in the section 4.1. The memory consumption of each filter after implementation in the hardware platform is given below.

Complementary filter:

Flash used: 24014 of 131072 bytes (18.3%).

SRAM used: 6008 of 16384 bytes (36.7%).

Kalman Filter:

Flash used: 26898 of 131072 bytes (20.5%).

SRAM used: 6336 of 16384 bytes (38.7%).

Complementary filter utilized 18.3% of total flash available where as Kalman filter utilized around 20.5%. As Kalman filter has predict and update steps, it was expected to consume more flash memory than the complementary filter. The RAM used by complementary filter was around 36.7% which is slightly less than Kalman filter RAM utilization at 38.7%.

Overall, the research concentrated on implementing complementary and Kalman filter algorithms in a low memory platform and the memory utilization shows that the filters were successfully executed using the available memory to obtain high precision pitch and roll angles.

5.2.4 Summary

As the results from roll and pitch angle calculation for both stationary and in-motion scenario showed that the convergence time as well as the detected angle range of Kalman filter was better than the complementary filter. The complementary filter, being a simple filter among the two, might be the light-weight algorithm on the calculation front, but it could not eliminate all the errors generated from sensors. On the other hand, the Kalman filter being an iterative algorithm with predict and update steps could yield a better result of roll and pitch angles while the device was both stationary and in motion. The Kalman filter could eliminate the errors arising from the sensors more efficiently. The raw accelerometer sensor values were quick to converge with the predefined angles of the experiment in all cases, but suffered from errors in both stationary and in-motion scenarios. The raw gyroscope sensor data showed the rate of change of angle, hence it could not be considered in the analysis of these algorithms. The memory utilization also showed that the research was able to implement the complementary and Kalman filter in a hardware platform with a low memory consumption and obtained a high precision roll and pitch angles.

5.3 Advantages and Limitations

This section covers the benefits and limitations of the research. This research was aimed at calculating a high precision roll and pitch angles when the hardware setup used has a limited computation power and memory. The hardware setup used in this research had a low computation power, but the research work was successful in configuring multiple complex filters such as complementary and Kalman in same hardware setup at the same time. Also, the testing results prove the initial understanding of Kalman filter performance.

The toy train might not look like an optimal setup to measure the roll and pitch angles of an aircraft. But, the main goal was to analyze the complementary filter and the Kalman filter algorithms by using the readily available accelerometer and gyroscope sensor data, and incorporate them in these filters to obtain high precision roll and pitch values. It is ultimately experimenting the algorithms with various angles and scenarios. Once an efficient algorithm is decided with these experiment results, the same algorithm could be fine-tuned to fetch similar performance if the experiments were performed in an aircraft. Hence, the most important step in this research was to consider all the different possible angles and scenarios at which the experiment could be performed in a controlled setup. This was achieved by using the IMU mounted on a toy train to replicate the vibrations , which in turn inserts error and noise in the sensors. Using the toy train in the experiments was cost effective as well. The testing of algorithms in an aircraft would have lead to a massive cost in performing the experiments, as the complementary and Kalman filter algorithms have several parameters that would have to be configured based on the experimental conditions. Performing multiple experiments in an aircraft would be very costly just for fine tuning the parameters of the algorithms.

Chapter 6

Conclusion

The goal of the research is to analyze the performance using a complementary filter or a Kalman filter to estimate the roll/pitch of an aircraft. The hardware setup included two sensors - an accelerometer and a gyroscope. Accelerometer provides the acceleration of an object in motion in relation to gravity and a gyroscope measures the rate of change of angle, also termed as an angular velocity [6]. But, these sensor outputs suffer from errors due to the force and acceleration on an accelerometer as well as drift errors on a gyroscope. Hence, the filters such as a complementary filter or a Kalman filter can be applied to these sensor values to eliminate the errors and obtain a precise pitch and roll estimation. When the Kalman filter was explored in detail, there was a matrix called covariance of error in sensor measurement (R matrix) using which the trust in sensor measurements could be changed. Hence, the research initially investigated the impact of this matrix on roll and pitch estimation in order to find a proper matrix for our extensive experiments. Followed by this first part of research, a performance analysis of complementary filter and Kalman filter was made for stationary and in-motion scenarios involving different predefined angles.

6.1 Detailed Conclusion

The covariance matrix for error in sensor measurement is a 2X2 matrix which can be initialized diagonally to help the mathematical calculations [4]. In total, a set of five different values of R matrix were analyzed to understand the behaviour of the Kalman filter. These values were chosen based on the behaviour of IMU and prior research work [33], [34], [35], [36]. Both the pitch and roll experiments were performed by configuring the R matrix at the angle of 45 degrees. This angle is used as an example to set a baseline to perform the experiments.

The summary of R matrix effect on Kalman filter is shown in the figures 6.1 and 6.2 for roll and pitch angles respectively. Small values of R matrix shows a quick convergence time (in seconds) with the predefined angle, but suffers from high sensitivity. This can be seen from having a high standard deviation. Higher values of R matrix makes the Kalman filter slow in converging to the predefined angle. But the output from the filter is stable as seen by smaller values of standard deviation.

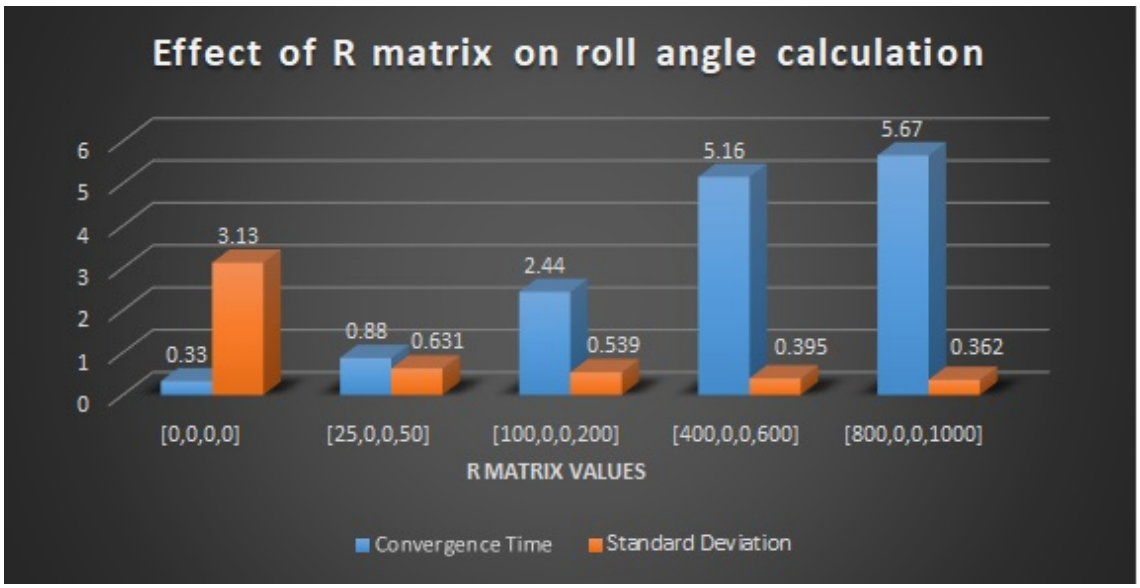

Figure 6.1: Effect of R matrix values on roll angle calculation of Kalman filter

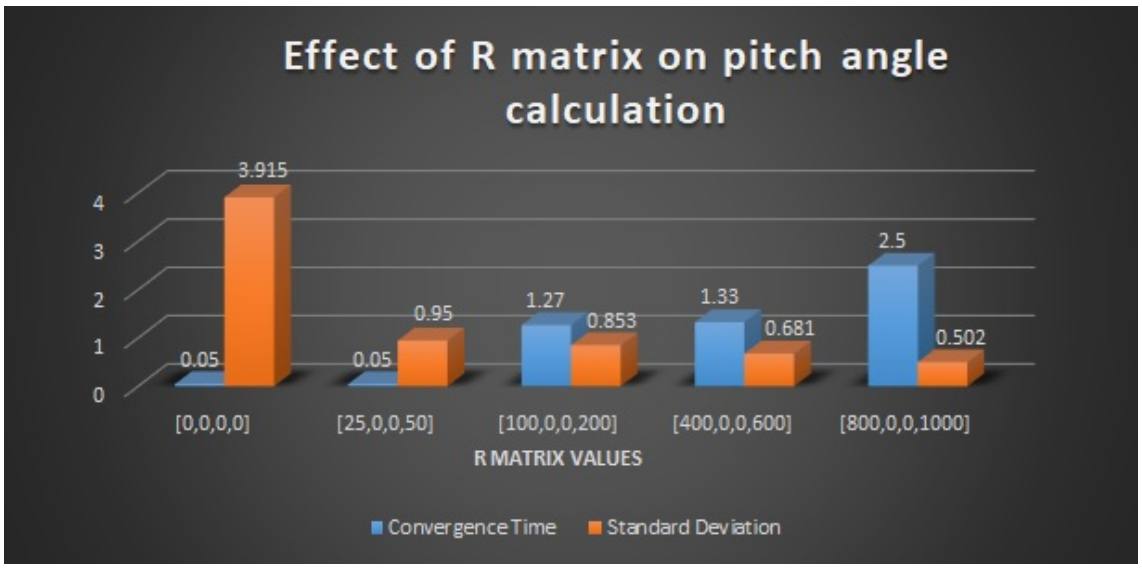

Figure 6.2: Effect of R matrix values on pitch angle calculation of Kalman filter

As the second part of research, the performance of complementary filter and a Kalman filter was thoroughly analyzed. In total, there were 16 experiments that were carried out to analyze the performance of complementary filter and Kalman filter with predefined angles as the baseline. Analysis of the filters was divided based on two scenarios : stationary and in-motion for both pitch and roll angle calculation. In the stationary scenario, both roll and pitch angle experiments showed that the Kalman filter was quick to reach the predefined angle along with the baseline of raw accelerometer measurements. But, the raw accelerometer sensor values suffered from errors which is shown by small deflections even in stationary scenario where there was no movement. The in-motion scenario impacted accelerometer sensor with severe errors which are evident from the graphs (figures 5.7 to 5.10 and figures 5.15 to 5.18) which shows lot of deflections when the accelerometer sensor data was plotted. Complementary filter was slow compared to Kalman filter and always took more time to converge to the predefined angle in all cases of pitch and roll angle calculations. Also, the output from Kalman filter was more stable compared to the output from complementary filter which proves the noise removal capcity of Kalman filter is better than complementary filter. Standard deviation was calculated for the output from both the filters also showed the roll and pitch angles measured by Kalman filter were more closer to the mean. From these experiments, it was evident that Kalman filter could produce high precision roll and pitch angles in both stationary and in-motion scenarios, when a similar research methodology is followed.

6.2 Future Work

There are multiple items in pipeline as the upcoming plan in this research. A aircraft device manufacturing company - Airbly Inc, situated in Charlottetown, PEI, Canada has agreed to test the solution proposed in this research in a real world scenario using a private aircraft. This opens up an excellent opportunity for the further research. As per the latest communication with the company, the testing results might be available by August 2019. Once the results are gathered, a further analysis of Kalman filter can be made with fine tuning the R matrix parameters to

obtain a precise roll and pitch angle. In this stage, we are also planning to explore more R matrix values to gain a better understanding of its impact on Kalman filter. Also, the raw accelerometer and the raw gyroscope data collection with the hardware setup used in this research in an actual aircraft can be further analyzed to apply any other type of filters to obtain an optimal solution suitable for processors with limited computation and memory. There is also a plan to calculate the yaw angle using the existing sensors in the hardware setup which can also be tested in different scenarios used in this research. The yaw angle calculation can also be verified in the real world scenario as the plan is to integrate it with the existing solution before the roll and pitch calculation is tested in a private aircraft.

Bibliography

[1] T. Islam, M. S. Islam, M. Shajid-Ul-Mahmud, and M. Hossam-E-Haider, "Comparison of complementary and kalman filter based data fusion for attitude heading reference system," in *AIP Conference Proceedings*, vol. 1919, no. 1. AIP Publishing, 2017, p. 020002.

[2] T. S. Institution, "Roll, pitch, and yaw." [Online]. Available: https://howthingsfly.si.edu/flight-dynamics/roll-pitch-and-yaw

[3] W. T. Higgins, "A comparison of complementary and kalman filtering," *IEEE Transactions on Aerospace and Electronic Systems*, no. 3, pp. 321–325, 1975.

[4] N. Thacker and A. Lacey, "Tutorial: The kalman filter," *Imaging Science and Biomedical Engineering Division, Medical School, University of Manchester*, p. 61, 1998.

[5] M. H. Ang and V. D. Tourassis, "Singularities of euler and roll-pitch-yaw representations," *IEEE Transactions on Aerospace and Electronic Systems*, no. 3, pp. 317–324, 1987.

[6] Y. S. Suh, "Orientation estimation using a quaternion-based indirect kalman filter with adaptive estimation of external acceleration," *IEEE Transactions on Instrumentation and Measurement*, vol. 59, no. 12, pp. 3296–3305, 2010.

[7] S. A. Salman, A. G. Sreenatha, and J. Y. Choi, "Attitude dynamics identification of unmanned aircraft vehicle," *International Journal of Control Automation and Systems*, vol. 4, no. 6, p. 782, 2006.

[8] H. Rehbinder and X. He, "Nonlinear pitch and roll estimation for walking robots," in *Proceedings 2000 ICRA. Millennium Conference. IEEE International Conference on Robotics and Automation. Symposia Proceedings (Cat. No. 00CH37065)*, vol. 3. IEEE, 2000, pp. 2617–2622.

[9] A. M. Sabatini, C. Martelloni, S. Scapellato, and F. Cavallo, "Assessment of walking features from foot inertial sensing," *IEEE Transactions on biomedical engineering*, vol. 52, no. 3, pp. 486–494, 2005.

[10] G. Welch and E. Foxlin, "Motion tracking survey," *IEEE Computer graphics and Applications*, vol. 22, no. 6, pp. 24–38, 2002.

[11] D. Gebre-Egziabher, G. H. Elkaim, J. Powell, and B. W. Parkinson, "A gyro-free quaternion-based attitude determination system suitable for implementation using low cost sensors," in *Position Location and Navigation Symposium*, 2000, pp. 185–192.

[12] R. P. Kornfeld, R. J. Hansman, and J. J. Deyst, "Single-antenna gps-based aircraft attitude determination," *Navigation*, vol. 45, no. 1, pp. 51–60, 1998.

[13] R. C. Hayward, D. Gebre-Egziabher, M. Schwall, J. D. Powell, and J. Wilson, "Inertially aided gps based attitude heading reference system (ahrs) for general aviation aircraft," in *Proceedings of the Institute of Navigation ION-GPS Conference*, 1997, pp. 1415–1424.

[14] R. Hayward, A. Marchick, and J. D. Powell, "Single baseline gps based attitude heading reference system (ahrs) for aircraft applications," in *Proceedings of the 1999 American Control Conference (Cat. No. 99CH36251)*, vol. 5. IEEE, 1999, pp. 3655–3659.

[15] G. Wahba, "A least squares estimate of satellite attitude," *SIAM review*, vol. 7, no. 3, pp. 409–409, 1965.

[16] I. Bar-Itzhack and Y. Oshman, "Attitude determination from vector observations: Quaternion estimation," *IEEE Transactions on Aerospace and Electronic Systems*, no. 1, pp. 128–136, 1985.

[17] I. Y. Bar-Itzhack and M. Idan, "Recursive attitude determination from vector observations euler angle estimation," *Journal of Guidance, Control, and Dynamics*, vol. 10, no. 2, pp. 152–157, 1987.

[18] R. E. Kalman, "A new approach to linear filtering and prediction problems," *Journal of basic Engineering*, vol. 82, no. 1, pp. 35–45, 1960.

[19] T. W. Wright, *Elements of mechanics including kinematics, kinetics and statics, with applications*. D. Van Nostrand Company, 1898.

[20] H. Hemami, "A state space model for interconnected rigid bodies," *IEEE Transactions on Automatic Control*, vol. 27, no. 2, pp. 376–382, 1982.

[21] R. P. Paul, *Robot manipulators: mathematics, programming, and control: the computer control of robot manipulators*. Richard Paul, 1981.

[22] M. J. Caruso, "Applications of magnetic sensors for low cost compass systems," in *Position Location and Navigation Symposium*, 2000, pp. 177–184.

[23] T. Ozyagcilar, "Implementing a tilt-compensated ecompass using accelerometer and magnetometer sensors," *Freescale semiconductor, AN*, vol. 4248, 2012.

[24] R. F. Tinder, "Relativistic flight mechanics and space travel," *Synthesis lectures on engineering*, vol. 1, no. 1, pp. 1–140, 2006.

[25] R. E. Mayagoitia, A. V. Nene, and P. H. Veltink, "Accelerometer and rate gyroscope measurement of kinematics: an inexpensive alternative to optical motion analysis systems," *Journal of biomechanics*, vol. 35, no. 4, pp. 537–542, 2002.

[26] R. E. Kalman and R. S. Bucy, "New results in linear filtering and prediction theory," *Journal of basic engineering*, vol. 83, no. 1, pp. 95–108, 1961.

[27] M. Euston, P. Coote, R. Mahony, J. Kim, and T. Hamel, "A complementary filter for attitude estimation of a fixed-wing uav," in *2008 IEEE/RSJ International Conference on Intelligent Robots and Systems*. IEEE, 2008, pp. 340–345.

[28] A. M. Sabatini, "Quaternion-based extended kalman filter for determining orientation by inertial and magnetic sensing," *IEEE Transactions on Biomedical Engineering*, vol. 53, no. 7, pp. 1346–1356, 2006.

[29] G. Buskey, J. Roberts, P. Corke, P. Ridley, and G. Wyeth, "Sensing and control for a small-size helicopter," in *Experimental robotics VIII*. Springer, 2003, pp. 476–486.

[30] S. Salcudean, "A globally convergent angular velocity observer for rigid body motion," *IEEE transactions on Automatic Control*, vol. 36, no. 12, pp. 1493–1497, 1991.

[31] J. Thienel and R. M. Sanner, "A coupled nonlinear spacecraft attitude controller and observer with an unknown constant gyro bias and gyro noise," *IEEE Transactions on Automatic Control*, vol. 48, no. 11, pp. 2011–2015, 2003.

[32] R. G. Brown, P. Y. Hwang *et al.*, *Introduction to random signals and applied Kalman filtering*. Wiley New York, 1992, vol. 3.

[33] L. Helge, "Pitch and roll estimating kalman filter for stabilizing quadrocopters – lhelge," 2012. [Online]. Available: https://lhelge.se/2012/04/pitch-and-roll-estimating-kalman-filter-for-stabilizing-quadrocopters/

[34] Alegiaco, "Kalman filter vs complementary filter _2011," 2011. [Online]. Available: https://robottini.altervista.org/kalman-filter-vs-complementary-filter

[35] Jannson, "simple-kalman-filter.c," Apr 2014. [Online]. Available: https://gist.github.com/jannson/9951716

[36] S. K. Rajagopalan, "sensor_fusion_ekf_imu," Aug 2018. [Online]. Available: https://github.com/syamprasadkr/sensor_fusion_ekf_imu

[37] T. S. Yoo, S. K. Hong, H. M. Yoon, and S. Park, "Gain-scheduled complementary filter design for a mems based attitude and heading reference system," *Sensors*, vol. 11, no. 4, pp. 3816–3830, 2011.

[38] R. Mahony, T. Hamel, and J.-M. Pflimlin, "Nonlinear complementary filters on the special orthogonal group," *IEEE Transactions on automatic control*, vol. 53, no. 5, pp. 1203–1217, 2008.

[39] T. Hamel and R. Mahony, "Attitude estimation on so [3] based on direct inertial measurements," in *Proceedings 2006 IEEE International Conference on Robotics and Automation, 2006. ICRA 2006.* IEEE, 2006, pp. 2170–2175.

[40] J. Kim, "Autonomous navigation for airborne applications," Ph.D. dissertation, Department of Aerospace, Mechanical and Mechatronic Engineering, Graduate, 2004.

[41] D. Choukroun, I. Y. Bar-Itzhack, and Y. Oshman, "Novel quaternion kalman filter," *IEEE Transactions on Aerospace and Electronic Systems*, vol. 42, no. 1, pp. 174–190, 2006.

[42] C. W. Kang and C. G. Park, "Attitude estimation with accelerometers and gyros using fuzzy tuned kalman filter," in *2009 European Control Conference (ECC).* IEEE, 2009, pp. 3713–3718.

[43] Y. Li, M. Efatmaneshnik, A. Cole, and A. G. Dempster, "Performance evaluation of ahrs kalman filter for mojortk system," in *Proceedings of International Global Navigation Satellite Systems Society IGNSS Symposium.* Citeseer, 2009.

[44] M. Wang, Y. Yang, R. R. Hatch, and Y. Zhang, "Adaptive filter for a miniature mems based attitude and heading reference system," in *PLANS 2004. Position Location and Navigation Symposium (IEEE Cat. No. 04CH37556).* IEEE, 2004, pp. 193–200.

[45] D. Gebre-Egziabher, R. C. Hayward, and J. D. Powell, "A low-cost gps/inertial attitude heading reference system (ahrs) for general aviation applications," in *IEEE 1998 Position Location and Navigation Symposium (Cat. No. 98CH36153).* IEEE, 1996, pp. 518–525.

[46] ——, "Design of multi-sensor attitude determination systems," *IEEE Transactions on aerospace and electronic systems*, vol. 40, no. 2, pp. 627–649, 2004.

[47] F. L. Markley, J. Crassidis, and Y. Cheng, "Nonlinear attitude filtering methods," in *AIAA Guidance, Navigation, and Control Conference and Exhibit*, 2005, p. 5927.

[48] S. K. Hong, "Fuzzy logic based closed-loop strapdown attitude system for unmanned aerial vehicle (uav)," *Sensors and Actuators A: Physical*, vol. 107, no. 2, pp. 109–118, 2003.

[49] ——, "Compensation of nonlinear thermal bias drift of resonant rate sensor using fuzzy logic," *Sensors and actuators A: physical*, vol. 78, no. 2-3, pp. 143–148, 1999.

[50] S. Hong and S. Park, "Minimal-drift heading measurement using a mems gyro for indoor mobile robots," *Sensors*, vol. 8, no. 11, pp. 7287–7299, 2008.

[51] D. G. Kim and S. K. Hong, "The compensation of nonlinear thermal bias drift of resonant rate sensor (rrs) using fuzzy logic," in *Proceedings of the IEEE 1998 National Aerospace and Electronics Conference. NAECON 1998. Celebrating 50 Years (Cat. No. 98CH36185)*. IEEE, 1998, pp. 38–42.

[52] R. Mahony, T. Hamel, and J.-M. Pflimlin, "Complementary filter design on the special orthogonal group so (3)," in *Proceedings of the 44th IEEE Conference on Decision and Control*. IEEE, 2005, pp. 1477–1484.

[53] R. Kottath, P. Narkhede, V. Kumar, V. Karar, and S. Poddar, "Multiple model adaptive complementary filter for attitude estimation," *Aerospace Science and Technology*, vol. 69, pp. 574–581, 2017.

[54] A. Mohamed and K. Schwarz, "Adaptive kalman filtering for ins/gps," *Journal of geodesy*, vol. 73, no. 4, pp. 193–203, 1999.

[55] R. Kottath, S. Poddar, A. Das, and V. Kumar, "Window based multiple model adaptive estimation for navigational framework," *Aerospace Science and Technology*, vol. 50, pp. 88–95, 2016.

[56] S. Romaniuk and Z. Gosiewski, "Kalman filter realization for orientation and position estimation on dedicated processor," *acta mechanica et automatica*, vol. 8, no. 2, pp. 88–94, 2014.

[57] G. Creamer, "Spacecraft attitude determination using gyros and quaternion measurements," *The Journal of the Astronautical Sciences*, vol. 44, no. 3, pp. 357–371, 1996.

[58] G. T. Haupt, N. J. Kasdin, G. M. Keiser, and B. W. Parkinson, "Optimal recursive iterative algorithm for discrete nonlinear least-squares estimation," *Journal of guidance, control, and dynamics*, vol. 19, no. 3, pp. 643–649, 1996.

[59] E. Foxlin, "Inertial head-tracker sensor fusion by a complimentary separate-bias kalman filter," in *vrais*. IEEE, 1996, p. 185.

[60] B. Barshan and H. F. Durrant-Whyte, "Evaluation of a solid-state gyroscope for robotics applications," *IEEE Transactions on Instrumentation and measurement*, vol. 44, no. 1, pp. 61–67, 1995.

[61] B. Friedland, "Treatment of bias in recursive filtering," *IEEE Transactions on Automatic Control*, vol. 14, no. 4, pp. 359–367, 1969.

[62] J. K. Hall, N. B. Knoebel, and T. W. McLain, "Quaternion attitude estimation for miniature air vehicles using a multiplicative extended kalman filter," in *2008 IEEE/ION Position, Location and Navigation Symposium*. IEEE, 2008, pp. 1230–1237.

[63] D. B. Barber, J. D. Redding, T. W. McLain, R. W. Beard, and C. N. Taylor, "Vision-based target geo-location using a fixed-wing miniature air vehicle," *Journal of Intelligent and Robotic Systems*, vol. 47, no. 4, pp. 361–382, 2006.

[64] F. L. Markley, "Attitude error representations for kalman filtering," *Journal of guidance, control, and dynamics*, vol. 26, no. 2, pp. 311–317, 2003.

[65] G. F. Welch and G. Bishop, "Scaat: Incremental tracking with incomplete information," Ph.D. dissertation, University of North Carolina at Chapel Hill, 1996.

[66] H. Qi and J. B. Moore, "Direct kalman filtering approach for gps/ins integration," *IEEE Transactions on Aerospace and Electronic Systems*, vol. 38, no. 2, pp. 687–693, 2002.

[67] S. Bancroft, "An algebraic solution of the gps equations," *IEEE Transactions on Aerospace and Electronic Systems*, no. 1, pp. 56–59, 1985.

[68] J. W. Chaffee and J. S. Abel, "The gps filtering problem," in *IEEE PLANS 92 Position Location and Navigation Symposium Record*. IEEE, 1992, pp. 12–20.

[69] K. Schwarz, M. Wei, and M. Van Gelderen, "Aided versus embedded-a comparison of two approaches to gps/ins integration," in *Proceedings of 1994 IEEE Position, Location and Navigation Symposium-PLANS'94*. IEEE, 1994, pp. 314–322.

[70] D. Cao, Q. Qu, C. Li, and C. He, "Research of attitude estimation of uav based on information fusion of complementary filter," in *2009 Fourth International Conference on Computer Sciences and Convergence Information Technology*. IEEE, 2009, pp. 1290–1293.

[71] H.-p. ZHANG and J.-c. FANG, "Short-time drift characteristic of mems gyroscope," *Journal of Chinese inertial technology*, vol. 1, 2007.

[72] J. Liu, R. Li, X. Niu, and L. Qiao, "Mems-based inertial integrated navigation technology for micro air vehicles," in *AIAA Guidance, Navigation, and Control Conference and Exhibit*, 2006, p. 6547.

[73] J. Tu, J.-J. Miau, Y. Wang, G. Lee, and C. Lin, "Studying three-dimensionality of vortex shedding at reynolds numbers of 10000 with mems sensors," in *44th AIAA Aerospace Sciences Meeting and Exhibit*, 2006, p. 1413.

[74] S. Zihajehzadeh, D. Loh, M. Lee, R. Hoskinson, and E. Park, "A cascaded two-step kalman filter for estimation of human body segment orientation using mems-imu," in *2014 36th Annual International Conference of the IEEE Engineering in Medicine and Biology Society*. IEEE, 2014, pp. 6270–6273.

[75] X. Yun and E. R. Bachmann, "Design, implementation, and experimental results of a quaternion-based kalman filter for human body motion tracking," NAVAL POSTGRADUATE SCHOOL MONTEREY CA DEPT OF ELECTRICAL AND COMPUTER ENGINEERING, Tech. Rep., 2006.

[76] J. K. Lee and E. J. Park, "Minimum-order kalman filter with vector selector for accurate estimation of human body orientation," *IEEE Transactions on Robotics*, vol. 25, no. 5, pp. 1196–1201, 2009.

[77] ——, "A fast gauss-newton optimizer for estimating human body orientation," in *2008 30th Annual International Conference of the IEEE Engineering in Medicine and Biology Society*. IEEE, 2008, pp. 1679–1682.

[78] H. J. Luinge and P. H. Veltink, "Measuring orientation of human body segments using miniature gyroscopes and accelerometers," *Medical and Biological Engineering and computing*, vol. 43, no. 2, pp. 273–282, 2005.

[79] J. K. Lee, E. J. Park, and S. N. Robinovitch, "Estimation of attitude and external acceleration using inertial sensor measurement during various dynamic conditions," *IEEE transactions on instrumentation and measurement*, vol. 61, no. 8, pp. 2262–2273, 2012.

[80] "Apple." [Online]. Available: https://support.apple.com/kb/SP685?locale=en_US

Appendix A

R Matrix Evaluation - Individual Results

A.1 Pitch Angle Calculation

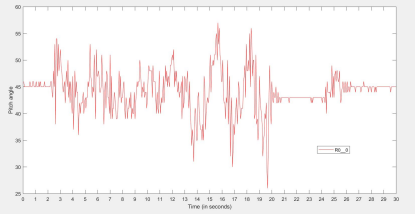

(a) *Pitch.R*0_0

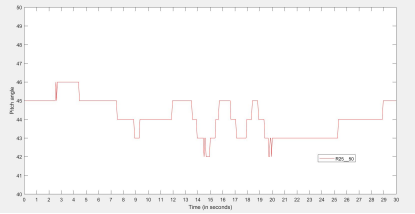

(b) *Pitch.R*25_50

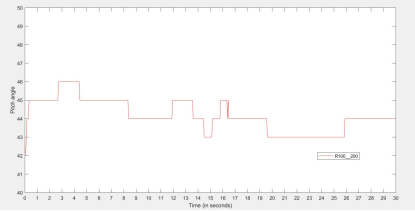

(c) *Pitch.R*100_200

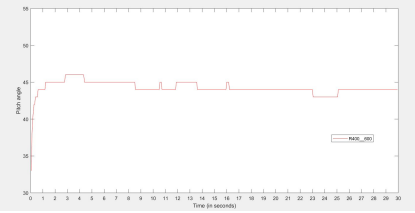

(d) *Pitch.R*400_600

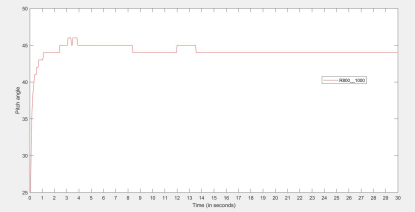

(e) *Pitch.R*800_1000

These are the individual test results from pitch angle experiment R matrix evaluation. As explained in section 5.2.1, the sensitivity of the Kalman filter decreases as the R matrix values increases. It is evident from the above figures as well. With the predefined angle of 45 degrees, the sensitivity increases as R matrix values increases. The first figure has the maximum amount of variations where the R matrix values were completely eliminated. In the next figures, Kalman filter becomes more stable as R matrix values increases.

A.2 Roll Angle Calculation

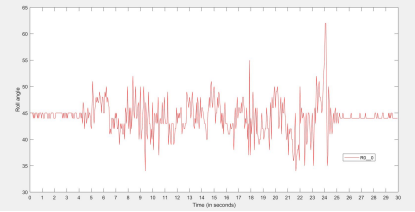

(a) *Roll*.*R*0_0

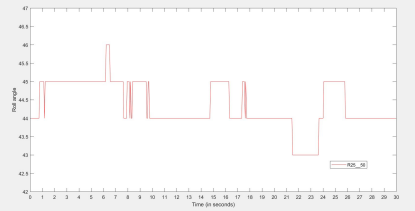

(b) *Roll*.*R*25_50

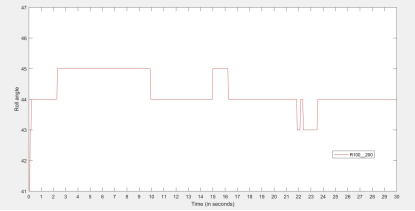

(c) *Roll*.*R*100_200

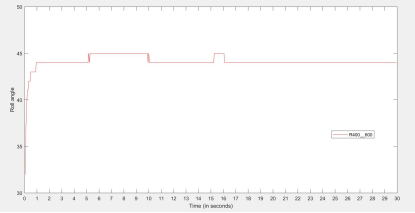

(d) *Roll*.*R*400_600

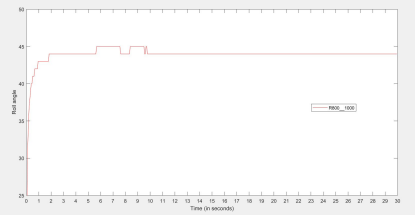

(e) *Roll*.*R*800_1000

These are the individual test results from roll angle experiment R matrix evaluation. As explained in section 5.2.2, the sensitivity of the Kalman filter decreases as the R matrix values increases. It is evident from the above figures similar to pitch angle experiment. The predefined angle is 45 degrees. The first figure has the maximum amount of variations where the R matrix values were completely eliminated. In the following figures, the Kalman filter becomes more stable as the R matrix values increases.